6. APPENDIX I

Micro volume voltammetric determination of 4-nitrophenol in dimethyl sulfoxide at a glassy carbon electrode

Gajdár Július, Barek Jiří, Fojta Miroslav, Fischer Jan

Monatshefte für Chemie - Chemical Monthly

Year 2017, Volume 148, Pages 1639-1644

Monatsh Chem (2017) 148:1639–1644
DOI 10.1007/s00706-017-1954-4

ORIGINAL PAPER

Micro volume voltammetric determination of 4-nitrophenol in dimethyl sulfoxide at a glassy carbon electrode

Július Gajdár[1] · Jiří Barek[1] · Miroslav Fojta[2] · Jan Fischer[1]

Received: 27 January 2017 / Accepted: 5 March 2017 / Published online: 1 July 2017

Abstract This study presents a miniaturized instrumentation for the determination of a model electrochemically reducible compound, 4-nitrophenol, in micro volumes of dimethyl sulfoxide at the glassy carbon electrode. Several working configurations of a three-electrode system and different constructions of reference electrodes are described. Moreover, the problem of the removal of oxygen (which is rather difficult in micro volumes) complicating the determination by differential pulse voltammetry, especially in a cathodic potential range was successfully solved. It has been found that the interference of oxygen can be partly eliminated by square wave voltammetry which is less sensitive to the presence of oxygen in the sample. Special apparatus capable of removing dissolved oxygen from 20 mm^3 of solution was also constructed and tested. It was verified that 4-nitrophenol can be determined in micro volumes of dimethyl sulfoxide by square wave voltammetry in the presence of dissolved oxygen (limit of quantification LOQ = 6.0 μmol dm^{-3}) and by differential pulse voltammetry after the removal of dissolved oxygen (LOQ = 2.4 μmol dm^{-3}). Both those methods are comparable with the determination in a macro volume (5.0 cm^3), which has LOQ = 1.3 μmol dm^{-3}.

Graphical abstract

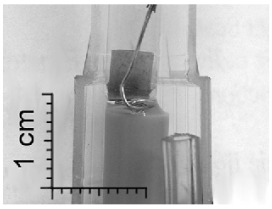

Keywords Square wave voltammetry · Differential pulse voltammetry · 4-Nitrophenol · Glassy carbon electrode · Dimethyl sulfoxide · Microanalysis

✉ Jan Fischer
jan.fischer@natur.cuni.cz

[1] UNESCO Laboratory of Environmental Electrochemistry, Department of Analytical Chemistry, Faculty of Science, Charles University, Albertov 6, 12843 Prague 2, Czech Republic

[2] Institute of Biophysics of the CAS, v. v. i., Královopolská 135, 61265 Brno, Czech Republic

Introduction

Recently great attention is paid to the miniaturization in the field of chemical and biochemical analysis with a goal to develop rapid, cheap, and sensitive methods with low cost and easy fabrication of necessary equipment. Voltammetric methods are especially suitable for these purposes as demonstrated by the review [1] summarizing various techniques, microelectrode designs, and fabrication methods. Combination of voltammetric methods and micro-analytical systems can be used for practical applications, e.g. analysis of small biochemical samples and they can also be used for in situ analysis, point-of-care testing, portable devices or lab-on chip devices [1, 2]. Moreover, this approach is frequently used in the development of electrochemical sensors [3–5]. Screen-printed electrodes (SPE) are most frequently used for

this type of work (analysis of micro volumes of samples). They are used as cheap and reliable single-use sensors [6, 7]. However, majority of commercially made SPEs are unsuitable for a work in organic solvents because the material from which they are made can be dissolved by those solvents [8].

Oxygen is present in dimethyl sulfoxide (DMSO) solutions in the range of 10^{-4} mol dm^{-3} and it is reduced in couple steps in aprotic solvents like DMSO, the first process is a reversible one-electron formation of superoxide anion radicals and the second irreversible process forms peroxide anions [9, 10]. Current response of oxygen dominates the cathodic potential range, resulting in the need of displacing oxygen with nitrogen or argon in the case of studying electrochemically reducible substances [11]. It was reported that the use of AC polarography/voltammetry with high frequencies (around 300 Hz) can circumvent the de-airing process because usually a studied species exhibits reversible behaviour and the wave current is increasing at a rate proportional on a square root of a frequency, however, oxygen reduction as an irreversible process increases its wave current at much slower rate [12]. Parameters of square wave voltammetry (SWV) can influence the current response of both reversible and irreversible processes. Low SWV response to irreversible systems diminishes negative influence and interference of oxygen [13]. Low detection limits combined with fast sweep rates (in the range of hundreds of mV s^{-1}) make SWV one of the most frequently applied methods for electrochemical studies [14].

4-Nitrophenol was chosen as a simple organic reducible substance and one of priority environmental pollutants that had been extensively studied by voltammetric methods on mercury [15], amalgam [16, 17], bismuth film [18], or glassy carbon [19] electrodes. Reduction of 4-nitrophenol or other nitrobenzene-like structures in aprotic solvents such as dimethyl sulfoxide is a two-step reaction with one-electron reversible reduction (to give anion radical) followed by three-electron irreversible reduction (to form hydroxylamine) at more negative potentials [20–22].

The aim of this work is to develop and test simple instrumentations for voltammetric measurements at the glassy carbon electrode (GCE) suitable for the work with a single drop (20 mm^3) of samples in organic solvents like DMSO and to develop the measuring protocol for the determination of model analyte 4-nitrophenol in micro volumes of samples. Special attention was paid to the matter of removal and non-removal of dissolved oxygen from the measured solutions and to the comparison of the newly developed miniaturized method with the standard macro volume determination.

Results and discussion

Configuration of electrodes for work in micro volumes

Several working miniaturized electrode configurations for the determination of 4-nitrophenol in micro volumes of 0.1 mol dm^{-3} tetrabutylammonium tetrafluoroborate (Bu_4NBF_4) in DMSO were constructed (see Fig. 1). Bulky GCE oriented upside down and platinum wire auxiliary electrode were always used. All electrodes and other equipments were fixated by external holders. Different reference electrode configurations are shown in Fig. 1a–c. Silver wire was used as a reference electrode in Fig. 1a. A non-aqueous reference electrode: silver wire in silver nitrate and supporting electrolyte dissolved in DMSO: Ag|0.01 mol dm^{-3} $AgNO_3$, 0.1 mol dm^{-3} Bu_4NBF_4; separated from the measured solution by a frit is used in Fig. 1b. Further development of this construction has led to a reference electrode connected to the solution with a salt bridge of supporting electrolyte in Luggin capillary [23]: Ag|0.01 mol dm^{-3} $AgNO_3$, 0.1 mol dm^{-3} Bu_4NBF_4|0.1 - mol dm^{-3} Bu_4NBF_4 (in DMSO) (see Fig. 1c). Arrangement suitable for removing dissolved oxygen from the solution was constructed as follows: the electrodes were positioned inside a plastic pipe with its ends insulated and a tube with the stream of nitrogen was positioned in the lower end of the plastic pipe (Fig. 1d). Described arrangements were reproducibly constructed while producing similar voltammetric responses. Nitrogen was beforehand passed through DMSO to saturate the gas with the solvent vapours and to minimize the evaporation of a micro volume of a sample solution, which could lead to the significant change of analyte concentration during measurements.

Comparison of the different reference electrode arrangements (Fig. 1a–c) is illustrated on cyclic voltammetric (CV) measurements in 20 mm^3 of solution in the presence of oxygen (see Fig. 2), which gave one signal at around −0.9 V corresponding to the reversible reduction to the superoxide anion radical, then at more negative potential −2.6 V a reduction of the peroxide anion was observed. The wide in-between peak (around −1.3 to −2.1 V) difficult to evaluate should therefore correspond to the irreversible reduction of the superoxide anion radical to the peroxide anion. Measurements with the silver wire reference electrode that were carried out beforehand in a macro volume were highly dependent on a degree of submersion of a wire into a solution which was demonstrated by the shift of the potential window as high as 0.3 V when comparing two extreme cases, one where the wire is only touching the surface of the solution and another one where

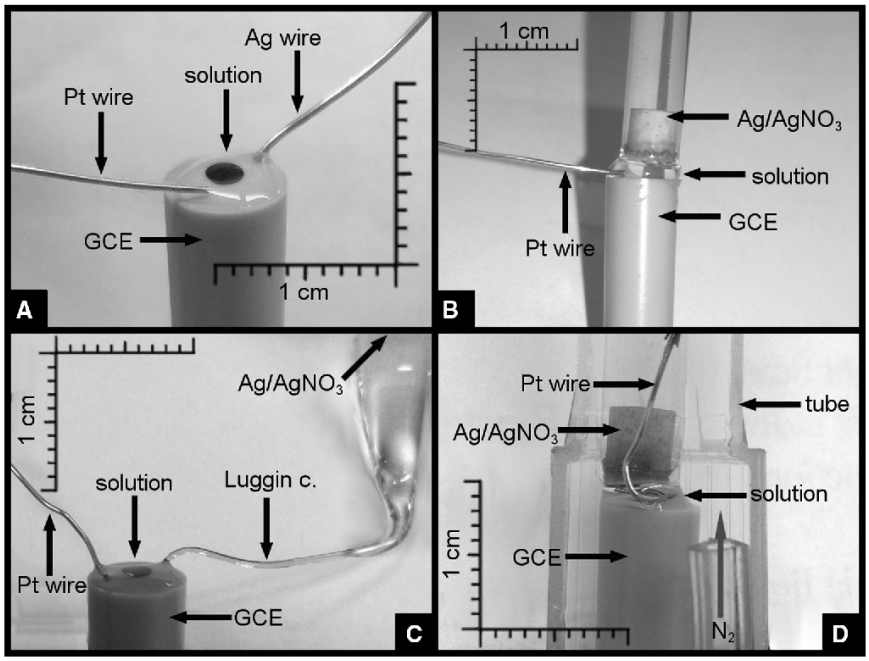

Fig. 1 Miniaturized configurations for the work in micro volumes (20 mm^3) with the glassy carbon electrode (GCE), platinum wire auxiliary electrode (Pt wire), and reference electrodes: **a** silver wire reference electrode (Ag wire), **b** Ag|0.01 mol dm^{-3} $AgNO_3$, 0.1 mol dm^{-3} Bu_4NBF_4 in DMSO reference electrode with frit, and **c** reference electrode connected to the solution with Luggin capillary through salt bridge Ag|0.01 mol dm^{-3} $AgNO_3$, 0.1 mol dm^{-3} Bu_4NBF_4|0.1 mol dm^{-3} Bu_4NBF_4 (all in DMSO). **d** Arrangement for the work in the nitrogen atmosphere inside a plastic pipe with highlighted direction of the nitrogen stream

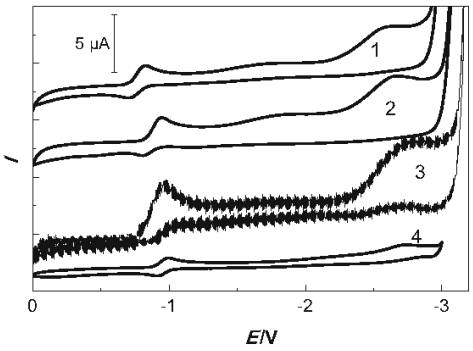

Fig. 2 Cyclic voltammograms (scan rate 100 mV s^{-1}) obtained at the GCE in 20 mm^3 of the supporting electrolyte 0.1 mol dm^{-3} Bu_4NBF_4 in DMSO in the presence of dissolved oxygen (three reduction waves) with platinum wire auxiliary electrode and with three different constructions of reference electrodes: Ag wire electrode (*curve 1*, see Fig. 1a), Ag|0.01 mol dm^{-3} $AgNO_3$, 0.1 mol dm^{-3} Bu_4NBF_4 (*curve 2*, see Fig. 1b) and Ag|0.01 mol dm^{-3} $AgNO_3$, 0.1 mol dm^{-3} Bu_4NBF_4|0.1 mol dm^{-3} Bu_4NBF_4 in Luggin capillary (*curve 3*, see Fig. 1c). Cyclic voltammogram in a macro volume solution with Ag|0.01 mol dm^{-3} $AgNO_3$, 0.1 mol dm^{-3} Bu_4NBF_4 reference electrode is depicted for the sake of comparison (*curve 4*)

the wire is submerged 1 cm deep into the solution. The position or the depth of submersion of the platinum wire auxiliary electrode did not have any observable effect on voltammetric measurements. CVs with the silver wire and Ag|0.01 mol dm^{-3} $AgNO_3$, 0.1 mol dm^{-3} Bu_4NBF_4 reference electrodes were equivalent (Fig. 2, curves 1 and 2) to voltammograms recorded in the macro volume (Fig. 2, curve 4). CV with the reference electrode connected with the measured solution through Luggin capillary (Fig. 2, curve 3) was considerably different. Periodic oscillations were observed in voltammograms and according to references [24–27] this phenomenon is observed on these types of reference electrodes positioned in a vicinity of a working electrode. For this type of configuration to work successfully it is necessary to precisely investigate the effect of positioning of all three electrodes, which is a far more complex problem outside the scope of this work and it might not be the best option for the analytical application in micro volumes with this type of arrangement. In all cases, no signal for silver ions from the reference electrode filling solution was observed near approx. −0.5 V, meaning that neither of these reference electrodes contaminated the analysed samples.

Determination of 4-nitrophenol

To evaluate the proposed arrangements, a model analyte 4-nitrophenol was at first determined by classic differential pulse voltammetry (DPV) in a macro volume (5 cm^3). These measurements had provided a base for the comparison of proposed miniaturized methods. 4-Nitrophenol gave two signals in 0.1 mol dm^{-3} Bu_4NBF_4 in DMSO after the removal of dissolved oxygen: one around −0.95 V and another higher signal at more negative potential −1.9 V, in agreement with the mechanism of reaction described in the introduction and in [20–22]. At the lowest measureable concentration range 10^{-6} - mol dm^{-3} 4-nitrophenol was determined by evaluating the peak at −1.9 V and this method gave a limit of quantification (LOQ) 1.3 μmol dm^{-3}.

For measurements in micro volumes of 0.1 mol dm^{-3} Bu_4NBF_4 in DMSO the arrangement depicted in Fig. 1b was employed because it proved to be the most reliable and provided the most stable results. Non-removal of dissolved oxygen in the micro volume greatly influenced parameters of the determination. The peak at around −0.95 V was overlapped by several times higher oxygen peak (at around −0.9 V) and was not practically observable, even at high concentrations of 4-nitrophenol. Second peak at around −1.9 V was observable only at higher concentrations of 4-nitrophenol because the peak coincided with the wide peak (around −1.3 to −2.1 V) caused by dissolved oxygen (see Fig. 3, curve 2), and that resulted in lower sensitivity and about tenfold higher LOQ compared to the macro volume determination (Table 1).

Two approaches for solving this problem were further investigated. One is the special arrangement shown in Fig. 1d constructed to achieve nitrogen atmosphere inside a plastic pipe. The process of removing dissolved oxygen is, however, much slower presumably because oxygen is removed only at the surface of a liquid and its transport to this surface is secured only by slow diffusion processes in an unstirred solution. It took about 15–20 min to remove the oxygen to the extent it did not interfere with the determination of 4-nitrophenol at −1.9 V. The oxygen peak at around −0.9 V was still present (Fig. 3). It is also important to mention that removing oxygen from DMSO is a difficult and lengthy process even in macro volume measurements. It usually takes around 10 min to completely remove dissolved oxygen, compared to aqueous solutions where 5-min purging with nitrogen is routinely used. DPV in 20 mm^3 of DMSO after 15 min in the nitrogen atmosphere is illustrated in Fig. 4. The calibration curve has a considerable intercept value, but parameters like sensitivity and LOQ shown in Table 1 are comparable with the determination in the macro volume. Peak potential shifts with the increasing concentration of 4-nitrophenol in the calibration dependency (Fig. 4) are noticeable; however, this was also observed in the macro volume and it is most probably caused by an electrode–analyte interaction and not by the miniaturization of the method.

Second tested approach was the determination using SWV which was tried out to minimize the negative influence of dissolved oxygen. Parameters of SWV like frequency, modulation amplitude, and potential step were optimized. The frequency was found to be the most important factor, whereas the amplitude and the potential step have influenced the peak to noise ratio only slightly. The optimal frequency was found to be 100 Hz when the height of 4-nitrophenol peak at around −1.9 V to the height of the oxygen peak at around −0.9 V ratio reached maximum at 1:2.5 (see dotted line at curve 1, Fig. 3). Further increase of the frequency has led to the unfavourable decrease of 4-nitrophenol peak. For comparison, the peak of analyte to the oxygen peak ratio was 1:5 (see dotted line at curve 2, Fig. 3) in DPV in the presence of dissolved oxygen and 2:1 (see dotted line at curve 3, Fig. 3) in favour of the analyte when working in the nitrogen atmosphere. This comparison is illustrated in Fig. 3, where it can also be seen that the current response of the wide peak caused by dissolved oxygen (around −1.3 to −2.1 V) that interfered with the DPV determination is also decreased when using the optimized SWV method. It can be also noted that in SWV both observable peak potentials (oxygen peak at −0.9 V and 4-nitrophenol at around −1.9 V) were unequally shifted to more positive potentials compared to DP voltammograms (whereas 4-nitrophenol peak shift was around +50 mV, oxygen peak shift was around +100 mV). This method has higher limit of quantification

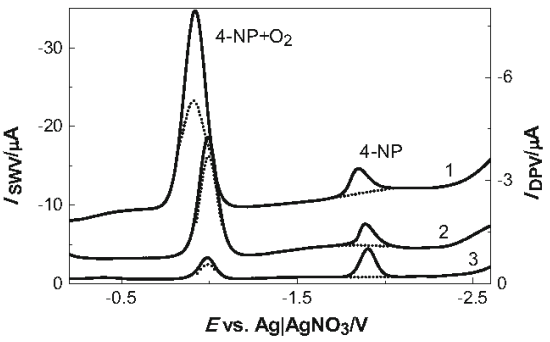

Fig. 3 Comparison of SWV and DPV curves for the determination of 4-nitrophenol (0.1 mmol dm^{-3}, 4-NP) at the GCE in 0.1 mol dm^{-3} Bu_4NBF_4 in DMSO in 20 mm^3 of the solution. SWV (frequency 100 Hz, pulse amplitude −50 mV, potential step −4 mV) (*curve 1*) and DPV (scan rate 20 mV s^{-1}, pulse amplitude −50 mV, pulse width 100 ms, sampling time 20 ms) (*curve 2*) curves in the presence of dissolved oxygen and DPV after 15 min in nitrogen atmosphere (*curve 3*). Supporting electrolyte voltammograms are illustrated as dotted lines in corresponding curves

than DPV method in the partly degassed solution but it is still considerably lower than DPV method in the presence of dissolved oxygen. The calibration dependency is linear in the investigated range (Table 1). However, as seen in Fig. 5, some deviation from a linearity is observed at high concentrations of 4-nitrophenol which is relatively common phenomenon in the case of solid electrodes.

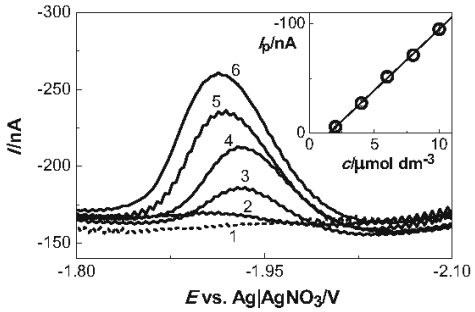

Fig. 4 DP voltammograms (conditions from Fig. 3) of 4-nitrophenol [0.0 (*1*); 2.0 (*2*); 4.0 (*3*); 6.0 (*4*); 8.0 (*5*); and 10.0 (*6*) μmol dm ^{3}] obtained at the GCE in 0.1 mol dm ^{3} Bu_4NBF_4 in DMSO in 20 mm^3 of the solution using the configuration shown in Fig. 1d after 15 min in the nitrogen atmosphere. Calibration curve is shown in the inset

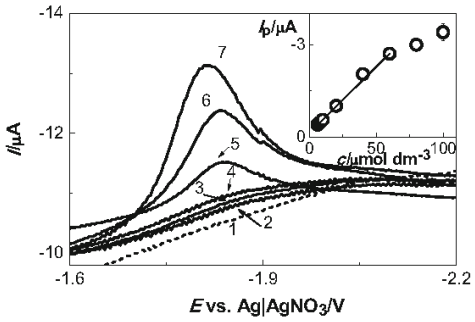

Fig. 5 SW voltammograms (conditions from Fig. 3) of 4-nitrophenol [0.0 (*1*); 6.0 (*2*); 8.0 (3); 10 (*4*); 20 (*5*); 40 (*6*); and 60 (*7*) μmol dm ^{3}]obtained at the GCE in 0.1 M Bu_4NBF_4 in DMSO in 20 mm^3 of the solution using the configuration shown on Fig. 1b. Calibration straight line for the range 6.0–60 μmol dm ^{3} is shown in the inset

Conclusion

Voltammetric determination of 4-nitrophenol at the GCE was successfully modified for the micro volume scale of a single drop (20 mm^3) of DMSO solutions. A few configurations of the three-electrode system were proved to be working except the configuration with Luggin capillary reference electrode which did not prove to be suitable. Two methods for determination of this analyte were proposed: SWV, which is capable of working without the necessity of removing dissolved oxygen, is more time efficient; and DPV, where a special construction was developed suitable for the work in the nitrogen atmosphere, is considerably more time-consuming but more sensitive.

Experimental

A stock solution of 1 mmol dm^{-3} 4-nitrophenol (CAS number: 100-02-7; ≥99%, Sigma Aldrich, Germany) was prepared by dissolving the substance in dimethyl sulfoxide (Penta, Czech Republic). More diluted solutions were prepared by exact dilution of the stock solution with DMSO. Tetrabutylammonium tetrafluoroborate (Bu_4NBF_4, p.a. Sigma Aldrich, Germany) was used as a supporting electrolyte in DMSO. Reference electrode filling solution was prepared with 0.01 mol dm^{-3} silver nitrate (p.a., Lachner, Czech Republic) and supporting electrolyte 0.1 mol dm^{-3} Bu_4NBF_4 in DMSO. All chemicals were used without further purification.

Instrumentation and procedures

All solutions for voltammetric measurements were prepared by measuring 1.0 cm^3 of 0.5 mol dm^{-3} Bu_4NBF_4 in DMSO into a 5.0 cm^3 volumetric flask. Afterwards,

Table 1 Comparison of parameters of calibration dependencies for the determination of the lowest measurable concentrations of 4-nitrophenol by DPV and SWV at the GCE with Ag|0.01 mol dm ^{3} $AgNO_3$, 0.1 mol dm ^{3} Bu_4NBF_4 reference electrode using the peak at around −1.9 V in 20 mm^3 of the analysed solution and by DPV in the macro volume solution

Method	Conc. range/μmol dm ^{3}	Slope/mA dm^3 mol ^{1}	Intercept/nA	Corr. coeff.	LOQ/μmol dm ^{3}
DPV (with O_2)	20–100	−8.97	+136	0.9990	20
SWV (with O_2)	6–60	−427	−139	0.9996	6.0
DPV (in N_2 atm.)	2–10	−11.2	+16.7	0.9999	2.4
DPV (macro volume)	1–10	−10.9	+4.63	0.9997	1.3

appropriate amount of the stock solution of 4-nitrophenol in DMSO was added and the flask was filled with DMSO to the mark. This solution was either transferred to a voltammetric cell for macro volume measurements and then purged with nitrogen for 10 min or a single drop (20 mm^3) of the solution was pipetted onto the upside down positioned GCE for micro scale measurements.

Voltammetric measurements were carried out in a three-electrode system with working glassy carbon disc electrode (GCE, 2 mm diameter, 6.1204.600, Metrohm, Switzerland), auxiliary platinum wire electrode (0.5 mm diameter), silver wire reference electrode (0.6 mm diameter) or a reference electrode Ag|$AgNO_3$ (0.01 mol dm^{-3}), Bu_4NBF_4 (0.1 mol dm^{-3}) in DMSO. GCE was polished prior to the series of measurements with aqueous slurry of alumina powder (1.1 μm) to mirror-like appearance. GCE was then sonicated for 30 s in methanol and then for 30 s in DMSO. Cyclic voltammetric (CV) measurements were carried out at a scan rate 100 mV s^{-1}. Differential pulse voltammetry (DPV) was carried out using scan rate 20 mV s^{-1}, pulse width 100 ms, sampling time 20 ms, and pulse amplitude −50 mV. Square wave voltammetry (SWV) was carried out at frequency 100 Hz, pulse amplitude −50 mV and potential step −4 mV. Measurements were carried out on Autolab PGSTAT101 (Metrohm) controlled by Nova 1.11.2 software (Metrohm). All voltammetric curves were recorded at least five times at the laboratory temperature. Peak heights were evaluated from the line connecting minima before and after the peak. All calculated parameters were evaluated with Origin software (OriginLab Corp., USA). Limits of quantification (LOQ) were calculated as a concentration corresponding to a tenfold of a standard deviation of ten subsequent measurements at the lowest measurable concentration [28].

Acknowledgements This research was financially supported by the Grant Agency of the Czech Republic (Project GA CR P206/12/G151).

References

1. Xu X, Zhang S, Chen H, Kong J (2009) Talanta 80:8
2. Barek J, Fischer J, Navratil T, Peckova K, Yosypchuk B, Zima J (2007) Electroanalysis 19:2003
3. Libansky M, Zima J, Barek J, Dejmkova H (2014) Electroanalysis 26:1920
4. Hájková A, Vyskočil V, Josypčuk B, Barek J (2016) Sens Actuators B 227:263
5. Tvrdikova J, Danhel A, Barek J, Vyskocil V (2012) Electrochim Acta 73:23
6. Renedo OD, Alonso-Lomillo MA, Martínez MJA (2007) Talanta 73:202
7. Wang J (1994) Analyst 119:763
8. Almeida ES, Silva LAJ, Sousa RMF, Richter EM, Foster CW, Banks CE, Munoz RAA (2016) Anal Chim Acta 934:1
9. Taitiro F, Kosuke I, Takeo A (1969) Bull Chem Soc Jpn 42:140
10. Koch TR, Purdy WC (1972) Talanta 19:989
11. Wojciechowski M, Go W, Osteryoung J (1985) Anal Chem 57:155
12. Bond AM (1973) Talanta 20:1139
13. Krause MS, Ramaley L (1969) Anal Chem 41:1365
14. Mirceski V, Gulaboski R, Lovric M, Bogeski I, Kappl R, Hoth M (2013) Electroanalysis 25:2411
15. Ni Y, Wang L, Kokot S (2001) Anal Chim Acta 431:101
16. Fischer J, Vanourkova L, Danhel A, Vyskocil V, Cizek K, Barek J, Peckova K, Yosypchuk B, Navratil T (2007) Int J Electrochem Sci 2:226
17. Niaz A, Fischer J, Barek J, Yosypchuk B, Sirajuddin, Bhanger MI (2009) Electroanalysis 21:1786
18. Hutton EA, Ogorevc B, Smyth MR (2004) Electroanalysis 16:1616
19. Pfeifer R, Martinhon PT, Sousa C, Moreira JC, do Nascimento MAC, Barek J (2015) Int J Electrochem Sci 10:7261
20. Andres T, Eckmann L, Smith DK (2013) Electrochim Acta 92:257
21. Zuman P, Fijalek Z, Dumanovic D, Suznjevic D (1992) Electroanalysis 4:783
22. Zuman P (1967) Substituent effects in organic polarography. Plenum Press, New York
23. Bott A (1995) Curr Sep 14:64
24. Eisenberg M, Tobias CW, Wilke CR (1955) J Electrochem Soc 102:415
25. Krischer K, Varela H, Bırzu A, Plenge F, Bonnefont A (2003) Electrochim Acta 49:103
26. Lee J, Christoph J, Strasser P, Eiswirth M, Ertl G (2001) J Chem Phys 115:1485
27. Birzu A, Green BJ, Otterstedt RD, Jaeger NI, Hudson JL (2000) Phys Chem Chem Phys 2:2715
28. Miller JN, Miller JC (2005) Statistics and chemometrics for analytical chemistry. Pearson Education Ltd., Harlow

7. APPENDIX II

Voltammetry of a novel antimycobacterial agent 1-hydroxy-*N*-(4-nitrophenyl)naphthalene-2-carboxamide in a single drop of a solution

Gajdár Július, Goněc Tomáš, Jampílek Josef, Brázdová Marie, Bábková Zuzana, Fojta Miroslav, Barek Jiří, Fischer Jan

Electroanalysis

Year 2018, Volume 30, Pages 38-47

Full Paper Wiley Online Library ELECTROANALYSIS

DOI: 10.1002/elan.201700547

Voltammetry of a Novel Antimycobacterial Agent 1-Hydroxy-*N*-(4-nitrophenyl)naphthalene-2-carboxamide in a Single Drop of a Solution

Július Gajdár[+],[a] Tomáš Goněc[+],[b] Josef Jampílek[+],[c] Marie Brázdová[+],[d] Zuzana Bábková[+],[d] Miroslav Fojta[+],[d] Jiří Barek[+],*[a] and Jan Fischer[+][a]

Abstract: The aim of this study is the development of a miniaturized voltammetric method for the determination of an antimycobacterial agent 1-hydroxy-*N*-(4-nitrophenyl)naphthalene-2-carboxamide (HNN) in a single drop (20 μL) of a solution by cathodic and anodic voltammetry at a glassy carbon electrode. Cyclic voltammetry was used to investigate its redox properties followed by the optimization of differential pulse voltammetric determination in a regular 10 mL volume. The optimal medium for the analytical application of both cathodic and anodic voltammetry was found to be Britton-Robinson buffer pH 7.0 and dimethyl sulfoxide (9:1, v/v). HNN gave one cathodic peak at around −0.6 V and one anodic peak at around +0.2 V vs. Ag|AgCl (3 mol L^{-1} KCl) reference electrode. Determination of HNN in a 10 mL volume gave the limit of quantification around 10 nmol L^{-1} by both adsorptive stripping anodic and cathodic voltammetry. Afterwards, miniaturized voltammetric methods in a single drop of solution (20 μL) were investigated. This approach requested some modifications of the cell design and voltammetric procedures. A novel method of removing dissolved oxygen in a single drop had to be developed and tested. Developed miniaturized voltammetric methods gave parameters comparable to the determination of HNN in 10 mL. The applicability of the miniaturized method was verified by the determination of HNN in a drop of a bacterial growth medium.

Keywords: Hydroxynaphthalene-2-carboxanilide · Microcell · Single drop analysis · Voltammetry

1 Introduction

The number of tuberculosis infections caused by the pathogen *Mycobacterium tuberculosis* has grown by 10 million cases with 1.4 million deaths in 2015 [1] with the most cases being from resource-poor countries with limited effectiveness of public health system and individuals with immunodeficiency virus HIV. In recent years this has been fuelled by emergence of drug resistant strains complicating the treatment that could take up to 24 months with the combination of eight to ten drugs [2]. Isoniazid, rifampicin, pyrazinamide, and ethambutol are used as first-line drugs. In addition, drug resistant strains are treated by second- or even third-line drugs such as fluoroquinolones, ethionamide, thioacetazone, linezolid, bedaquilline, delamanid, etc. [3] that are in general more toxic to organism. Thus, this situation necessitates the identification of new molecular scaffolds that offer shorter, more effective and less toxic compounds. Because of those reasons the development of new tuberculosis drugs has been very intensive in recent years [2].

One of the novel molecular scaffolds that were recently developed are hydroxynaphthalenecarboxamides [4–10]. Their structure is based on salicylanilides, second-line drugs. The synthesis and primary antibacterial and antimycobacterial activity of tens of derivatives was tested and compared with the first-line drugs like isoniazid and rifampicin. Most of them showed comparable or higher antimicrobial activity especially against resistant strains, with low toxicity to human leukemia cell lines. One of the compounds (1-hydroxy-*N*-(4-nitrophenyl)naphthalene-2-carboxamide; HNN) has been chosen for this pilot electroanalytical study. As it is a newly prepared compound no electrochemical studies have been carried out so far.

[a] J. Gajdár,[+] J. Barek,[+] J. Fischer[+]
Charles University, Faculty of Science, Department of Analytical Chemistry, UNESCO Laboratory of Environmental Electrochemistry, Albertov 6, CZ-12843 Prague 2, Czech Republic
E-mail: barek@natur.cuni.cz
[b] T. Goněc[+]
University of Veterinary and Pharmaceutical Sciences, Faculty of Pharmacy, Department of Chemical Drugs, Palackého 1/3, CZ-61242 Brno, Czech Republic
[c] J. Jampílek[+]
Comenius University, Faculty of Pharmacy, Department of Pharmaceutical Chemistry, Odbojárov 10, SK-83232 Bratislava, Slovakia
[d] M. Brázdová,[+] Z. Bábková,[+] M. Fojta[+]
Institute of Biophysics of the Czech Academy of Sciences, Královopolská 135, CZ-61265 Brno, Czech Republic
[+] This work was presented at the Modern Electrochemical Methods XXXVII conference (May 15–19 2017, Jetřichovice near Děčín, Czech Republic)

Voltammetric techniques are frequently applied in the development and validation of analytical methods for determination of pharmaceuticals in their formulations and various biological samples. They also provide a way to determine kinetic and mechanistic parameters which are valuable as an insight into metabolic reactions which is a matter of importance in the field of pharmaceutical or biological analysis [11–13]. Voltammetric determination is in some cases applicable directly in biological matrices without the lengthy extraction process. Voltammetric methods have been used for the determination of various biologically active substances on mercury and various solid and modified electrodes (see reviews [12,14]).

Microcells and microanalysis of small samples in the range of tenths to hundreds of microlitres have been present in the field of voltammetry for a long time. These microcells can be used as flow-through detectors coupled with chromatographic or flow injection analysis or they can work in batch arrangements with static samples introduced into the system by a pipette or other similar devices. There are two basic configurations of the working electrode in batch arrangements. It could be in its usual state set from top to bottom and immersed in a small volume sample. Other option is an inverted state set from bottom to top that favours possibility of applying even smaller volumes on the surface of the working electrode facing upwards [15]. A few microcell designs with carbon-based working electrodes were introduced in several studies [16–21]. Microcells can be developed and then used as portable devices, micro scale systems or for in vivo analysis with a simple and inexpensive instrumentation [22].

HNN contains electrochemically active reducible nitro group on the phenyl moiety and oxidizable hydroxyl group on the naphthyl moiety (see Figure 1). Structurally similar nitrobenzene-like structures have been intensively studied by voltammetric methods on glassy carbon electrodes [23–25] or by polarography in mixed *N,N*-dimethylformamide-water solutions [26]. One nitro group is usually reduced in one irreversible 4-electron process giving hydroxylamine structure in an aqueous medium even in the presence of some organic solvent [24,25,27,28].

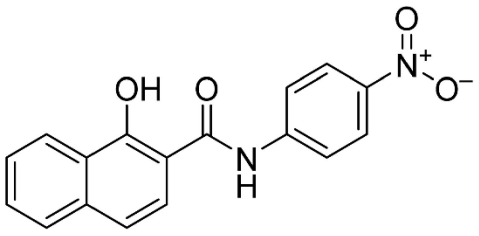

Fig. 1. Structural formula of 1-hydroxy-*N*-(4-nitrophenyl) naphthalene-2-carboxamide (HNN).

Hydroxyl group on the naphthyl moiety has been studied on glassy carbon [24,29] or boron doped diamond electrodes [30]. The oxidation of naphthol/phenol-based compounds starts with a deprotonation and one electron formation of an oxo-radical. This radical can then take part in various parallel reactions giving quinone derivatives or in some coupling reactions that create polymeric films unfortunately contributing to the electrode passivation [29–31]. In the study of niclosamide (structurally very similar to HNN) it is proposed that the compound is at first deprotonated and then oxidized by the loss of 2 electrons to form a bi-radical cation followed by an intermolecular cyclisation [32].

This work is based on our previous development of the miniaturized system for determination of 4-nitrophenol in dimethyl sulfoxide [33]. The goal of this study is to examine electrochemical properties of the novel antimycobacterial agent HNN and to optimize parameters for its determination focusing on the miniaturization of the electrochemical cell that is favourable for the work in small volumes of biological matrices. The newly developed miniaturized methods can be then easily used for the investigation of other novel antimycobacterial agents usually available only in very small amounts.

2 Experimental

2.1 Chemicals and Reagents

A stock solution of HNN (0.01 mol L^{-1}, 1-hydroxy-4′-nitro-2-naphthanilide; CAS number: 68352-27-2; Sigma Aldrich, Germany) was prepared by dissolving 15.41 mg of the substance in 5 mL of dimethyl sulfoxide (DMSO, p.a., Penta, Czech Republic). More diluted solutions were prepared by the exact dilution of the stock solution with DMSO. Britton-Robinson buffer was prepared by mixing 0.04 mol L^{-1} phosphoric, boric, and acetic acid with 0.1 mol L^{-1} sodium hydroxide (all p.a. Lach-ner, Czech Republic). The bacteria growth medium contained 0.4 mol L^{-1} sucrose (white refined granulated sugar, Investice Strategie Management a.s., Czech Republic), 0.02 mol L^{-1} phosphoric buffer pH 7.2 prepared by mixing disodium hydrogen phosphate and sodium dihydrogen phosphate (p.a. Lach-ner), 5 mmol L^{-1} sodium chloride (p.a. Lach-ner), and 15 mmol L^{-1} magnesium chloride (p.a. Lachema, Czech Republic). Deionised water was produced by Millipore Milli-Q system (Millipore, USA).

Stability of HNN stock solution was monitored spectrophotometrically at UV-vis spectrometer Agilent 8453 (Agilent, USA) by its absorbance peak at 351 nm. Stock solution was stable for at least one month.

2.2 Apparatus

Voltammetric measurements were carried out on Eco-Tribo Polarograph controlled by Polar Pro 5.1 software (both Polaro-Sensors, Czech Republic) in a three-electrode system with a working disc glassy carbon electrode

(GCE, 2 mm diameter, 6.1204.110 and 6.1204.600, Metrohm, Switzerland), an auxiliary platinum wire electrode (0.5 mm diameter), and a reference Ag|AgCl electrode (3 mol L^{-1} KCl; Elektrochemicke detektory, Turnov, Czech Republic) or a pseudo-reference silver wire electrode (0.6 mm diameter). pH measurements were conducted with pH-meter Jenway 3510 (Bibby Scientific Ltd, United Kingdom) with Jenway combined glass electrode (924005) calibrated using standard aqueous buffers.

Cyclic voltammetry (CV) was usually carried out at a scan rate 100 mV s^{-1} unless stated otherwise. Differential pulse voltammetry (DPV) was carried out using scan rate 20 mV s^{-1}, pulse width 100 ms, sampling time 20 ms, and pulse amplitude ±50 mV. All voltammetric curves were recorded at least 5 times at laboratory temperature. Peak heights were evaluated from the line connecting minima before and after the peak. Limits of quantification were calculated as a concentration corresponding to a tenfold of a standard deviation of ten subsequent measurements at the lowest measurable concentration [34].

2.3 Macro Volume Instrumentation and Procedures

Working electrode was polished prior to measurements with aqueous slurry of alumina powder (1.1 μm) on a polishing pad to a mirror-like appearance and then sonicated for 30 s in methanol and deionised water. The electrode was then carefully dried out with a cellulose swab. This was usually repeated after every 5 measurements by cathodic DPV and before every single measurement by anodic DPV unless stated otherwise.

Solutions were prepared by adding appropriate amount of the stock solution of HNN in DMSO into a 10.0 mL volumetric flask. Appropriate volume of DMSO was then added to achieve the final volume of the organic solvent in a given medium varying from 0.1 to 1 mL (v/v). Afterwards the flask was filled with BR buffer solution of given pH, 0.01 mol L^{-1} KCl solution or the bacterial growth medium to the mark. Obtained solution was transferred to a voltammetric cell. For cathodic measurements, 10 mL of the solution was then purged for 5 min with nitrogen saturated with deionised water and DMSO (9:1) vapours to prevent sample solution evaporation, and corresponding voltammogram was recorded. The purging was repeated for 30 s before every repeated measurement.

2.4 Microcell Instrumentation and Procedure

Microcells used are depicted in Figure 2. Two different reference electrodes were used: first one was the Ag|AgCl electrode (Figure 2A); the second one was the silver wire pseudo-reference electrode (Figure 2B). The plastic tube was manufactured from the 5 mL pipette tip cut to the appropriate size and carefully melted at the ends to form curved edges around electrodes to better isolate nitrogen atmosphere inside. A hole was cut to the side for a nitrogen input. Before experiments the reference electrode and the auxiliary electrode were fixated by holders while plastic tube could be moved up and down. Before every measurement reference and auxiliary electrodes were washed with a few drops of DMSO and deionised water. Pre-treated GCE was then positioned opposite the reference electrode and 20–50 μL drop of a solution was carefully pipetted in-between electrodes. The plastic tube was slid over the drop resting on the external holder as depicted in Figure 2. Oxygen was removed from the solution by passing nitrogen through this set-up for 10–20 mins depending on the measurement conditions. Nitrogen was at first saturated with the deionised water and DMSO (9:1) vapours to minimize the evaporation of the sample drop. In the case of anodic voltammetry oxygen removal was not necessary. Therefore, plastic tube in depicted configurations was not used.

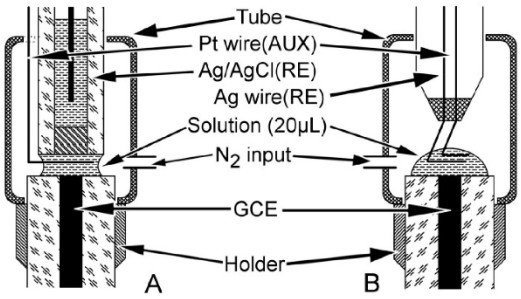

Fig. 2. Microcells used for measurements in 20–50 μL of a solution with a working GCE, a reference Ag|AgCl electrode (A) or a pseudo-reference electrode (B), a platinum wire auxiliary electrode and a plastic tube used only for cathodic voltammetry designed to achieve nitrogen atmosphere inside the microcell.

3 Results and Discussion

3.1 Electrochemical Study of HNN in Macro Volume (10 mL)

Because of HNN's very limited solubility in water, mixed buffer – DMSO solutions had to be used. Maximum content of DMSO based on biological studies of this compound [4–10] was around 10% (v/v) and this is the percentage mostly used throughout this study. However, even in this 10% DMSO medium, HNN was soluble only in neutral and alkaline media at the concentration 10 μmol L^{-1} which is necessary for acceptably high CV peaks. Therefore, voltammetry of HNN was not studied at pH lower than 6.0.

3.1.1 Mechanism of HNN Reduction

The reduction of HNN was studied by CV in the BR buffer pH 7 – DMSO medium (9:1) at GCE at the scan rate 100 mV s^{-1} (see Figure 3b). HNN gave one irreversible reduction peak I at −594 mV. In the reverse scan the peak IIa at −90 mV is observed that together with the peak IIb at −106 mV, observed in the second cathodic

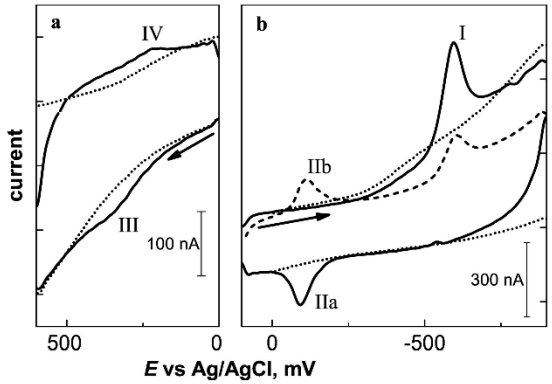

Fig. 3. Cyclic voltammograms (scan rate 100 mV s^{-1}) of HNN (c = 10 μmol L^{-1}) obtained at GCE in 10 mL of BR buffer pH 7.0 and DMSO (9:1, v/v) medium in the anodic range (a) and in the cathodic range (b). Supporting electrolyte is illustrated as dotted line. Dashed line in (b) denotes the second cathodic scan. Arrows denote the start and the direction of a scan.

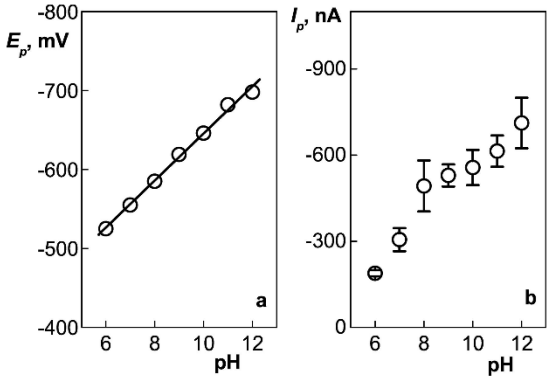

Fig. 4. Dependence of the cathodic peak potential (a) and the cathodic peak current (b) of HNN (c = 10 μmol L^{-1}) on pH of BR buffer obtained at GCE in 10 mL of BR buffer (pH 6.0–12.0) and DMSO (9:1, v/v) medium by DP voltammetry.

scan, forms reversible pair separated by 16 mV which is usually assigned to the reversible nitroso/hydroxylamino pair. The observed lower than theoretically expected peak potential difference (around 30 mV) can be explained by the adsorption phenomena (see later). In the series of scans, the height of the peak I decreased while heights of reversible peaks IIa/IIb were both increasing indicating a passivation of the electrode surface by the product of the reduction (I). The effect of various scan rates (20–400 mV s^{-1}) was studied to further characterise the electrode reaction. The height of the cathodic peak I was linearly dependant on the square root of the scan rate (R = 0.9953) confirming a diffusion controlled process. Similarly, the process (IIa) was diffusion controlled (R = 0.9914). However, the process (IIb) was adsorption controlled (R = 0.9940). The cathodic peak I was shifting to more negative potentials and the separation of the reversible pair IIa/IIb was growing with increasing scan rates which is a common observation at solid electrodes.

The potential of the cathodic peak I was monitored by DPV in BR buffer pH 6.0–12.0 and DMSO (9:1, v/v) media (see Figure 4a). The peak potential was shifted to more negative potentials with the slope −29.8 mV pH^{-1} in the studied range. The theoretical value for 4H$^+$/4e$^-$ reduction of nitro group to hydroxylamine is −59.1 mV pH^{-1} [35]. Experimental value corresponds to 1:2 (H$^+$:e$^-$) ratio, probably 2H$^+$/4e$^-$ reduction. The deviation from the theoretical value can be caused by the proton deficiency in neutral and alkaline media.

These observations are in an agreement with the reduction of nitroaromatics discussed in the literature which exhibit 4-electron irreversible reduction (peak I) of nitro group to hydroxylamine. The reversible pair (IIa/IIb) should therefore correspond to two electron hydroxyl-amine/nitroso reversible reaction [24,25,27,28].

3.1.2 Mechanism of HNN Oxidation

The anodic response of HNN was studied under same conditions. HNN gave one irreversible anodic peak III at +351 mV. In the reverse scan, a small peak IV at +219 mV was observed (see Figure 3a). In the series of scans the height of the peak III significantly decreased and its potential moved to more positive potentials while the height of the peak IV increased which could point to the adsorption of the product on the electrode surface. At increasing scan rates, the potential of the anodic peak III was shifted to more positive potentials while the position of the peak IV was constant. Dependency of the height of the anodic peak III on the scan rate and on the square root of the scan rate indicates involvement of both diffusion and adsorption as a controlling step of this process.

The change of the potential of the anodic peak III with pH of the BR buffer was studied by DPV (see Figure 5a). The peak potential was dependent on pH of BR buffer from 6.0 to 10.0 where it was shifting towards 0 V. However, in more alkaline solutions the peak potential remained constant at around +130 mV. In BR buffer pH 12.0 – DMSO medium (9:1) the second and the third peak are observed indicating that a different electrode mechanism was starting to take place. The potential of the peak III was dependent on pH of BR buffer with a slope −51.8 mV pH^{-1} (for pH 6.0–10.0). This means that the first step of the reaction is the deprotonation of the hydroxyl group. In the alkaline medium HNN was completely deprotonated and no protons were involved in a redox reaction (pH > 10.0). The intersection of linear parts of the plot in Figure 5a could be approximated as a dissociation constant of hydroxyl group [36] at around 9.7 in this specific BR buffer – DMSO medium (9:1).

The first step of the oxidation should therefore involve deprotonation leading to one electron process (peak III) to give oxo-radical compounds as is common in hydroxy-

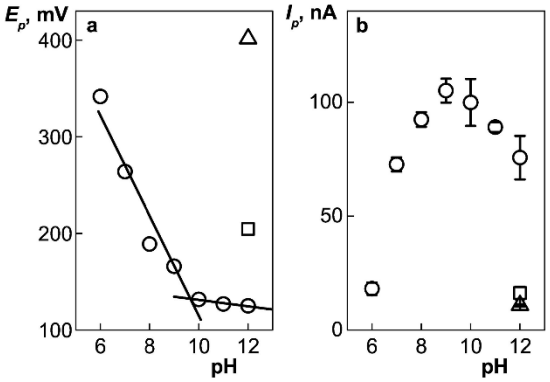

Fig. 5. Dependence of the anodic peak potential (a) and the anodic peak current (b) of HNN ($c = 10\ \mu mol\,L^{-1}$) on pH of BR buffer obtained at GCE in 10 mL of BR buffer (pH 6.0–12.0) and DMSO (9:1, v/v) medium by DP voltammetry.

aromatic compounds. They can then react in several parallel reactions also giving a polymeric film contributing to the electrode passivation in an agreement with literature [30,31].

3.1.3 Cathodic DP Voltammetry of HNN

As mentioned before, HNN gave one cathodic DPV peak corresponding to the CV peak I (Figure 1b). Dependence of the peak height on pH of the BR buffer (see Figure 4b) gave the highest peak in the BR buffer pH 12.0 – DMSO (9:1) medium. The adsorption of the product of the reduction at the GCE surface resulted in a large signal at the potential near 0 V (corresponding to the CV peak IIb) from the second scan onward on the pre-treated GCE. DPV peak (I) height continually decreased with the number of scans on the same electrode surface. However, it was found out that the decrease that occurs in 5 scans (RSD = 5 %, $c = 10\ \mu mol\,L^{-1}$) is acceptable for the determination especially since the electrode fouling was less intense at lower concentrations of HNN. Therefore, GCE had to be polished before each series of 5 measurements. The pre-treatment of the electrode in an ultrasonic bath in methanol for 30 s and deionised water for 30 s after polishing gave better repeatability than just polishing on an alumina pad and rinsing with deionised water. The calibration curve in this medium (see Table 1) had sigmoidal shape with the linear range only from 0.6 to 4 $\mu mol\,L^{-1}$.

Because one of the goals of this work is the development of the method for the determination of HNN in biological matrices, at the next step the determination was carried out in the BR buffer pH 7.0 – DMSO (9:1) medium as it can be safely assumed that most of the matrices of a biological origin will have pH around 7. The electrode fouling was observed as well and the same pre-treatment procedure was applied as in pH 12 with an acceptable deviation for 5 consequent scans with a slightly declining trend (RSD = 7 %, $c = 10\ \mu mol\,L^{-1}$). HNN gave a linear response in the range from 0.2 to 10 $\mu mol\,L^{-1}$ limited by its solubility (Table 1). In the end, the BR buffer pH 7.0 – DMSO (9:1) medium turned out to be

Table 1. Parameters of determination of HNN obtained at GCE in different media by cathodic (CDPV), anodic (ADPV), cathodic adsorptive stripping (CAdSDPV) and anodic adsorptive stripping (AAdSDPV) differential pulse voltammetry in 10 mL of a solution. The accumulation time t_{acc} is applicable only in AdSDPV.

Technique	medium	E_p, V	t_{acc}, s	c, mol L^{-1}	slope, mA L mol^{-1}	intercept, nA	corr. coef.	LOQ, mol L^{-1}
CDPV	BR buffer pH 12 – DMSO (9:1)	−0.70	–	$(6–40)\times10^{-7}$	−68.9	+22.7	0.9888	$\approx 8\times10^{-7}$
CAdSDPV	BR buffer pH 12 – DMSO (9:1)	−0.70	15	$(1–10)\times10^{-7}$	−70.5	−1.84	0.9993	1.3×10^{-7}
CAdSDPV	BR buffer pH 12	−0.65	60	$(4–40)\times10^{-8}$	−118	−4.55	0.9957	5.8×10^{-8}
CDPV	BR buffer pH 7 – DMSO (9:1)	−0.55	–	$(2–10)\times10^{-6}$	−21.1	−0.355	0.9992	–
CDPV	BR buffer pH 7 – DMSO (9:1)	−0.55	–	$(2–10)\times10^{-7}$	−30.8	−0.406	0.9980	2.2×10^{-7}
ADPV	BR buffer pH 7 – DMSO (9:1)	+0.26	–	$(1–10)\times10^{-6}$	+9.07	−1.68	0.9984	1.1×10^{-6}
CAdSDPV	0.01 M KCl – DMSO (9:1)	−0.55	60	$(2–10)\times10^{-8}$	−237	−2.46	0.9983	4.0×10^{-8}
CAdSDPV	0.01 M KCl – DMSO (99:1)	−0.55	1200	$(8–60)\times10^{-9}$	−1130	+1.57	0.9984	1.1×10^{-8}
AAdSDPV	BR buffer pH 7 – DMSO (9:1)	+0.26	60	$(1–10)\times10^{-7}$	+87.9	+2.65	0.9974	1.0×10^{-7}
AAdSDPV	BR buffer pH 7 – DMSO (99:1)	+0.26	1200	$(1–10)\times10^{-8}$	+1070	+0.032	0.9969	1.7×10^{-8}
CDPV	Bacterial growth medium pH 7.2	−0.56	–	$(2–10)\times10^{-6}$	−40.8	+9.35	0.9978	–
CDPV	– DMSO (9:1)	−0.56	–	$(2–10)\times10^{-7}$	−38.1	+2.73	0.9889	2.3×10^{-7}
ADPV		+0.25	–	$(1–10)\times10^{-6}$	+5.33	−0.549	0.9994	2.0×10^{-6}

more suitable medium for the determination of HNN by cathodic DPV.

3.1.4 Anodic DP Voltammetry of HNN

HNN gave one anodic peak (corresponding to the CV peak III, see Figure 1a) and its height was dependent on pH with the maximum in the BR buffer pH 9.0 – DMSO (9:1) medium (see Figure 5b). The anodic peak current was much lower than the cathodic response. The determination was firstly carried out in the BR buffer pH 7.0 – DMSO (9:1) medium. As it later turned out the determination at pH 9.0 would bring none or only minor benefits regarding the solubility of HNN or the peak height. The electrode fouling was also a problem in this case. Products of oxidation strongly passivated the electrode surface. The peak height was dramatically decreasing and the peak position was not stable in the series of measurements. Therefore, the electrode had to be polished before every single measurement to achieve acceptable repeatability (RSD = 7%, $N = 10$, $c = 10\ \mu mol\ L^{-1}$). HNN gave a linear response in the range from 1 to 10 μmol L^{-1} (Table 1).

3.1.5 Cathodic and Anodic DP Voltammetry of HNN in Bacterial Growth Medium

Pharmaceutical studies of this compound are only at the beginning and HNN was so far studied for its biological activity only in a few matrices listed here [4–10]. One of the matrices, a bacterial growth medium used for testing the inhibition of photosynthetic electron transport (PET), was thus chosen as the real sample. The expected concentration range of the analyte is from 0.1 to 1000 μmol L^{-1}. Using a developed cathodic and anodic voltammetric method for the BR buffer pH 7.0 – DMSO (9:1) medium, HNN exhibited the linear dynamic range from 0.2/2.0 (cathodic/anodic DPV, respectively) to 10 μmol L^{-1} in the medium with 10% DMSO content (see Figure 6 and Table 1). Higher concentrations of HNN (to 1000 μmol L^{-1}) would require higher DMSO content.

3.1.6 Cathodic Adsorptive Stripping DP Voltammetry of HNN

The determination by adsorptive stripping voltammetry was carried out at pH 12.0 and pH 7.0 of BR buffer (BR buffer at pH 7.0 was substituted for 0.01 mol L^{-1} KCl solution because of some impurities). The aim was to continually decrease the DMSO content as low as possible and continually increase the accumulation time. HNN showed very good adsorptive characteristics that could be correlated with its low solubility in water. The optimal accumulation potential in the 0.01 mol L^{-1} KCl and DMSO (9:1) medium was −0.1 V from the studied range (+0.1 V to −0.3 V). In the concentration range 10^{-8} mol L^{-1} HNN was determined with a short accumulation time 60 s in a stirred solution. Then, DMSO content

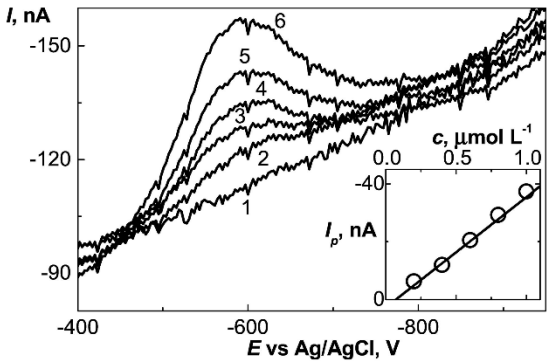

Fig. 6. Cathodic DP voltammograms of HNN (0.0 (1); 0.2 (2); 0.4 (3); 0.6 (4); 0.8 (5); 1.0 (6) μmol L^{-1}) obtained at GCE in 10 mL of the bacterial growth medium pH 7.2 and DMSO (9:1, v/v) medium. The calibration curve is shown in the inset.

was lowered to 1% and it was found out that further decreasing the DMSO content did not have any significant effect on the peak height (see Figure 7b). By increasing the accumulation time to 20 min (see Figure 7a) it was possible to detect HNN in nanomolar concentrations with the limit of quantification 1 nmol L^{-1} (Table 1). The solubility of HNN was experimentally determined by this method in deionised water at the laboratory temperature. The concentration of the saturated solution was determined as 22 (±3) nmol L^{-1}.

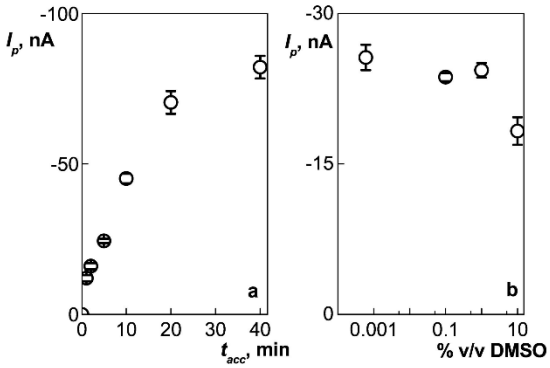

Fig. 7. Dependence of the peak height on the accumulation time t_{acc} (a) and the content of DMSO in a solution (in % v/v) (b) of HNN ($c = 60$ nmol L^{-1}) obtained at GCE in 10 mL of 0.01 mol L^{-1} KCl and DMSO (99:1, v/v) medium by the method of cathodic AdSDPV in a stirred solution at the accumulation potential −0.1 V.

The same procedure was applied in the BR buffer pH 12 – DMSO (9:1) medium. At the optimal accumulation potential 0.0 V and optimal accumulation time 15 s, it was possible to determine HNN in the linear range from 0.1 to 1 μmol L^{-1}. At this point, solubility of HNN was

experimentally determined in the medium containing only BR buffer pH 12. The concentration of the saturated solution was determined as 7.3 $(\pm 0.5) \times 10^{-7}$ mol L^{-1}. Using this solution as a stock solution and after increasing the accumulation time to 60 s (at the accumulation potential 0.0 V), the limit of quantification could be lowered to 58 nmol L^{-1} (Table 1). The increase of the accumulation time did not further improve determination parameters.

3.1.7 Anodic Adsorptive Stripping DP Voltammetry of HNN

These measurements were carried out only in the BR buffer pH 7.0 – DMSO (9:1) medium in the stirred solution. Previous findings from cathodic adsorptive voltammetric measurements were utilized. The optimal potential of accumulation was 0.0 V, and two values of accumulation times were used: 60 s (with 10% DMSO); and 20 min with lowered DMSO content (1%) (see Figure 8). In the latter case, the limit of quantification 17 nmol L^{-1} was reached (see Table 1).

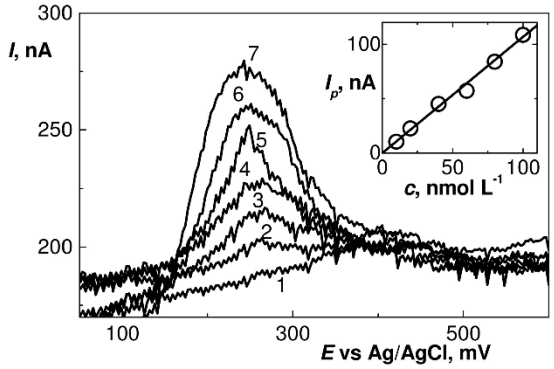

Fig. 8. Anodic AdSDP voltammograms of HNN (0.0 (1); 10 (2); 20 (3); 40 (4); 60 (5); 80 (6); and 100 (7) nmol L^{-1}) obtained at GCE after 20 min accumulation at the accumulation potential 0.0 V in 10 mL of BR buffer pH 7.0 and DMSO (99:1, v/v) medium in a stirred solution. The calibration curve is shown in the inset.

3.2 Electrochemical Study of HNN in a Single Drop of a Solution (20 µL)

After the optimization of the method in 10 mL volume, the BR buffer pH 7.0 and DMSO (9:1) medium was exclusively used. The working electrode pre-treatment was the same as in the macro volume. Microcells depicted in Figure 2 were used as described below.

3.2.1. Cathodic DP Voltammetry of HNN and Oxygen Removal

Miniaturization of the cathodic voltammetric method has brought a few problems that had to be solved. The first one was the removal of the negative influence of oxygen. Square wave voltammetry (SWV) was used in our previous work [33] because it is usually less sensitive to the presence of oxygen. However no positive effect of SWV was observed in this case. A similar arrangement was used as in the above mentioned study, but a few improvements had to be implemented. The plastic tube was manufactured to better isolate the inside of the microcell and the intake of nitrogen was drilled in a side of the tube with an intention of creating a slight over-pressure of nitrogen in the microcell. At first, the microcell from Figure 2A was used. The process of removing oxygen took around 15 minutes, presumably because in an unstirred drop the only transporting process present is a relatively slow diffusion.

However, while the removal of oxygen via diffusion took place, other diffusion processes occurred. HNN from the drop was adsorbed on the fritted glass of the reference electrode (HNN was already shown to be readily adsorbed from the solution) and it could also be slowly mixing with the reference electrode filling solution. HNN coming from the reference electrode back to the drop of the solution could thus influence subsequent measurements. This was overcome by using the silver wire as the pseudo-reference electrode (see Figure 2B). The use of the pseudo-reference electrode was limited to analytical purposes only as the potential of this electrode is somewhat unstable. This also shortened the time necessary for the complete removal of oxygen to 10 min as a relatively larger drop surface is in contact with the nitrogen atmosphere.

The amount of the compound that is depleted from the solution by electrolysis in one measurement is considered negligible in bulk analysis (10 mL) but it is considerable in a drop of a solution. One DPV scan had a significant impact on the concentration of HNN in the drop. It was calculated that a fast CV scan (scan rate 100 mV s^{-1}, $c = 10$ µmol L^{-1}) results in a 5% decrease of the concentration of HNN in the drop. Slower DPV scan (20 mV s^{-1}) presumably results in an even bigger decrease of the concentration. Therefore, only one measurement could be carried out in one drop. Because of that, the procedure for the determination of HNN was adapted accordingly. After the application of the drop, oxygen was being removed for 10 min during which time an accumulation of HNN on the electrode surface was occurring. Essentially, a method of adsorptive stripping voltammetry was thus used. The calibration curve was linear up to the concentration of 2 µmol L^{-1} (see Table 2). From this point on, the current height became much less reproducible with simultaneous decrease of the calibration curve slope. This can be contributed to the saturation of the electrode

Table 2. Parameters of the determination of HNN obtained at GCE in different media by cathodic (CDPV) and anodic (ADPV) differential pulse voltammetry, and cathodic adsorptive stripping differential pulse voltammetry (CAdSDPV) in a single drop of solution with the volume *V*. The accumulation time t_{acc} is identical with the time necessary for oxygen removal and is only applicable in CAdSDPV.

technique	medium	E_p, V	*V*, µL	t_{acc}, s	*c*, µmol L^{-1}	slope, mA L mol^{-1}	intercept, nA	corr. coef.	LOQ, mol L^{-1}
CDPV	BR buffer pH 7	−0.55	20	–	2–10	−11.9	+8.16	0.9970	–
CAdSDPV	– DMSO (9:1)	−0.55	20	600	0.1–2	−67.8	−2.22	0.9911	1.2×10^{-7}
ADPV		+0.26	20	–	1–10	+3.77	−0.518	0.9977	2.4×10^{-6}
CDPV	Bacterial growth medium pH 7.2	−0.56	20	–	2–10	−6.02	−2.51	0.9977	–
CAdSDPV	– DMSO (9:1)	−0.56	20	900	0.1–2	−54.7	−1.88	0.9901	1.2×10^{-7}
ADPV		+0.25	50	–	1–10	+5.25	−2.83	0.9977	2.2×10^{-6}

surface with adsorbed HNN as is frequently observed in AdSV.

HNN could be determined in a one drop at concentrations higher than 2 µmol L^{-1}. The signal height in second and further scans is stable enough and reasonably reproducible for 5 scans in the one drop on a new polished surface for an acceptable and reproducible determination at higher concentrations by DPV (see Table 2).

3.2.2 Cathodic DP Voltammetry of HNN in Bacterial Growth Medium

Determination of HNN by cathodic voltammetry was also carried out in a real sample of the bacterial growth medium. The microcell with the pseudo-reference electrode was used. The removal of nitrogen had to be lengthened to 15 minutes, probably caused by slower oxygen diffusion in a concentrated sucrose solution. Therefore, accumulation time was 15 min as well. In the lower concentration range HNN was determined by adsorptive voltammetry, and as observed in the buffered medium the saturation of the electrode surface occurred at around 2 µmol L^{-1} (see Figure 9). At higher concentrations, it was possible to determine HNN by DPV by 5 consecutive scans in one drop with acceptable signal stability (see Table 2).

3.2.3 Anodic DP Voltammetry of HNN

Anodic DPV determination was carried out in the same buffered medium: BR buffer pH 7.0 and DMSO (9:1). The working electrode had to be pre-treated before every single measurement because of the electrode fouling observed before in macro volumes. Depletion of HNN by electrolysis in a drop was not possible to observe because of the electrode fouling. The configuration of the microcell at Figure 2A was used without the plastic tube as the removal of oxygen was not necessary. The drop was pipetted onto the pre-treated GCE in the built microcell and a scan was performed immediately, therefore there was a little time for the drop of the solution mixing with the reference electrode filling solution and no cross-contamination was observed as it was the case in cathodic

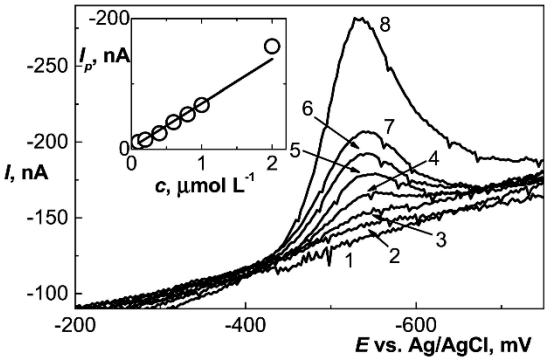

Fig. 9. Cathodic AdSDP voltammograms of HNN (0.0 (1); 0.1 (2); 0.2 (3); 0.4 (4); 0.6 (5); 0.8 (6); 1.0 (7); and 2.0 (8) µmol L^{-1}) obtained at GCE in 20 µL of bacterial growth medium pH 7.2 and DMSO (9:1, v/v) solution after 10 min accumulation under nitrogen atmosphere measured against silver wire pseudo-reference electrode (adjusted for Ag|AgCl in the figure). The calibration curve is shown in the inset.

DPV. The concentration dependency parameters are summarized in Table 2.

3.2.4 Anodic DP Voltammetry of HNN in Bacterial Growth Medium

Determination of HNN in a real matrix was also carried out by anodic DPV. The microcell (Figure 2A) was used and GCE was pre-treated before every voltammetric scan. However, in a drop of this medium splitting of the anodic peak was observed in some scans. The second peak appeared at more positive potential around +400 mV. To clarify, this was observed only in the bacterial growth medium – DMSO (9:1) and only in a drop (20 µL) of the solution and not in 10 mL. This splitting was observed only in some scans (about 50%) without any obvious trend in a series of measurements at the pre-treated GCE with the same solution but always with a newly applied drop.

With the addition of a surface-active compound such as Triton X100 from concentration 0.01% (v/v) it was possible to replicate the splitting even in 10 mL in every

scan. Addition of higher concentrations of Triton X100 shifted the height ratio of two peaks to the later one, but in 1% (v/v) Triton X100 solution a sensitivity of GCE determination decreased noticeably. It appears that surface-active compounds that could originate from impurities in the bacterial growth medium or from some working electrode handling process are then present in the drop which is particularly sensitive on their presence. The irreproducibility of the splitting of peaks could be attributed to the concentration of surface-active compounds in around critical levels and probably some fluctuation of their concentration could be occurring.

Another approach of circumventing this issue was to change the volume of the drop because, as described above, the splitting of the peak was not observed in 10 mL without the addition of Triton X100. A dependence of the double-peak occurrence on the volume of the drop of bacterial growth medium was investigated. It was found out that at the volume 50 µL the splitting was observed only in approx. 1 in 4 measurements; in 100 µL no splitting was observed but a drop of this volume is not suitable for the designed microcell. Therefore, a linear dependency was constructed with the drop volume 50 µL while scans with the obvious splitting were not evaluated (see Figure 10 and Table 1).

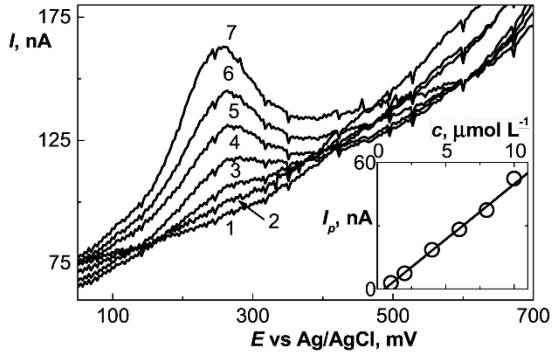

Fig. 10. Anodic DP voltammograms of HNN (0.0 (1); 1.0 (2); 2.0 (3); 4.0 (4); 6.0 (5); 8.0 (6); and 10.0 (7) µmol L^{-1}) obtained at GCE in 50 µL of bacterial growth medium pH 7.2 and DMSO (9:1, v/v) solution. The calibration curve is shown in the inset.

4 Conclusions

In this work, a successful miniaturization of the three-electrode cell for the determination of the novel antimycobacterial agent was introduced. HNN has been for the first time studied by cathodic and anodic voltammetry and its electrode mechanism was outlined. Some physical properties were also measured like the dissociation constant of the hydroxyl group in the studied medium pK(conditional) 9.7; HNN solubility in deionized water at 22 (±3) nmol L^{-1}; and in alkaline BR buffer pH 12.0 at 730 (±50) nmol L^{-1}. The optimal medium for the determination was found to be BR buffer pH 7.0 and 10% v/v (or lower) DMSO. The cathodic DPV current response of HNN was several times larger than the anodic response which was also reflected in limits of quantification: 0.2 µmol L^{-1} and 1 µmol L^{-1}, respectively. HNN was shown to have adsorptive properties and exploiting this observation has led to the lowest limit of quantification 11 nmol L^{-1} that was about equal for both anodic and cathodic AdSDPV. This compound was also successfully determined in a real matrix, the bacterial growth medium.

Miniaturization of developed methods gave rise to some problems that were successfully explained and overcome. The removal of oxygen was resolved by designing the microcell able of sustaining a nitrogen atmosphere inside. The contamination of the reference electrode with the analyte in cathodic DPV was overcome by using the silver wire as the pseudo-reference electrode. The depletion of the compound by electrolysis was solved by only applying one drop for one measurement on the pre-treated GCE. The splitting of the peak observed in the bacterial growth medium in anodic DPV was probably caused by surface-active compounds and a higher volume of the drop was then used for the determination of HNN to circumvent this problem. Parameters of determination were not significantly worse compared to the macro volume (10 mL).

This proposed miniaturized voltammetric cell can be used for the determination of other novel antimycobacterial agents or other electrochemically active compounds in microliters of samples for biological or pharmaceutical applications while it offers the same selectivity as it is characteristic to voltammetric methods.

Acknowledgements

Financial support of The Czech Science Foundation (project GA ČR P206/12/G151) is gratefully acknowledged.

References

[1] World Health Organisation, *Global tuberculosis report 2016*, WHO Press, Geneva, **2016**.
[2] A. Koul, E. Arnoult, N. Lounis, J. Guillemont, K. Andries, *Nature* **2011**, *469*, 483–490.
[3] Working Group on New TB Drugs 2017. Available online: http://newtbdrugs.org/pipeline/clinical (accessed on September 4 2017).
[4] T. Gonec, J. Kos, I. Zadrazilova, M. Pesko, R. Govender, S. Keltosova, B. Chambel, D. Pereira, P. Kollar, A. Imramovsky, J. O'Mahony, A. Coffey, A. Cizek, K. Kralova, J. Jampilek, *Molecules* **2013**, *18*, 9397–9419.
[5] T. Gonec, J. Kos, I. Zadrazilova, M. Pesko, S. Keltosova, J. Tengler, P. Bobal, P. Kollar, A. Cizek, K. Kralova, J. Jampilek, *Bioorg. Med. Chem.* **2013**, *21*, 6531–6541.
[6] T. Gonec, K. Kralova, M. Pesko, J. Jampilek, *Bioorg. Med. Chem. Lett.* **2017**, *27*, 1881–1885.
[7] T. Gonec, S. Pospisilova, T. Kauerova, J. Kos, J. Dohanosova, M. Oravec, P. Kollar, A. Coffey, T. Liptaj, A. Cizek, J. Jampilek, *Molecules* **2016**, *21*, 1068.

[8] T. Gonec, I. Zadrazilova, E. Nevin, T. Kauerova, M. Pesko, J. Kos, M. Oravec, P. Kollar, A. Coffey, J. Mahony, A. Cizek, K. Kralova, J. Jampilek, *Molecules* **2015**, *20*, 9767–9787.
[9] J. Kos, E. Nevin, M. Soral, I. Kushkevych, T. Gonec, P. Bobal, P. Kollar, A. Coffey, J. O'Mahony, T. Liptaj, K. Kralova, J. Jampilek, *Bioorg. Med. Chem.* **2015**, *23*, 2035–2043.
[10] J. Kos, I. Zadrazilova, M. Pesko, S. Keltosova, J. Tengler, T. Gonec, P. Bobal, T. Kauerova, M. Oravec, P. Kollar, A. Cizek, K. Kralova, J. Jampilek, *Molecules* **2013**, *18*, 7977–7997.
[11] J. Barek, J. Fischer, T. Navratil, K. Peckova, B. Yosypchuk, J. Zima, *Electroanalysis* **2007**, *19*, 2003–2014.
[12] Q. Xu, A. J. Yuan, R. Zhang, X. J. Bian, D. Chen, X. Y. Hu, *Curr. Pharm. Anal.* **2009**, *5*, 144–155.
[13] V. K. Gupta, R. Jain, K. Radhapyari, N. Jadon, S. Agarwal, *Anal. Biochem.* **2011**, *408*, 179–196.
[14] N. S. Lawrence, E. L. Beckett, J. Davis, R. G. Compton, *Anal. Biochem.* **2002**, *303*, 1–16.
[15] Y. I. Tur'yan, *Talanta* **1997**, *44*, 1–13.
[16] E. T. Smith, M. W. W. Adams, *Anal. Biochem.* **1992**, *207*, 94–99.
[17] K. Štulík, M. Štulíková, *Anal. Lett.* **1973**, *6*, 441–450.
[18] J. Wang, B. A. Freiha, *Anal. Chem.* **1982**, *54*, 334–336.
[19] J. O. Schenk, E. Miller, R. N. Adams, *Anal. Chem.* **1982**, *54*, 1452–1454.
[20] W. J. Bowyer, M. E. Clark, J. L. Ingram, *Anal. Chem.* **1992**, *64*, 459–462.
[21] M. Libansky, J. Zima, J. Barek, H. Dejmkova, *Electroanalysis* **2014**, *26*, 1920–1927.
[22] X. Xu, S. Zhang, H. Chen, J. Kong, *Talanta* **2009**, *80*, 8–18.
[23] R. Pfeifer, P. T. Martinhon, C. Sousa, J. C. Moreira, M. A. C. do Nascimento, J. Barek, *Int. J. Electrochem. Sci.* **2015**, *10*, 7261–7274.
[24] H. Alemu, P. Wagana, P. F. Tseki, *Analyst (Cambridge, U.K.)* **2002**, *127*, 129–134.
[25] T. Andres, L. Eckmann, D. K. Smith, *Electrochim. Acta* **2013**, *92*, 257–268.
[26] V. A. Ilina, S. S. Gitis, G. M. Galpern, N. N. Filatova, V. K. Shcheltsyn, *Zh. Anal. Khim.* **1975**, *30*, 574–578.
[27] P. Zuman, Z. Fijalek, D. Dumanovic, D. Suznjevic, *Electroanalysis* **1992**, *4*, 783–794.
[28] P. Zuman, *Substituent Effects in Organic Polarography*, Plenum Press, New York, **1967**.
[29] T. A. Enache, A. M. Oliveira-Brett, *J. Electroanal. Chem.* **2011**, *655*, 9–16.
[30] M. Panizza, P. A. Michaud, G. Cerisola, C. Comninellis, *J. Electroanal. Chem.* **2001**, *507*, 206–214.
[31] M. S. Ureta-Zanartu, P. Bustos, C. Berrios, M. C. Diez, M. L. Mora, C. Gutierrez, *Electrochim. Acta* **2002**, *47*, 2399–2406.
[32] H. Alemu, N. M. Khoabane, P. F. Tseki, *Bull. Chem. Soc. Ethiop.* **2003**, *17*, 95–106.
[33] J. Gajdár, J. Barek, M. Fojta, J. Fischer, *Monatsh. Chem.* **2017**, *148*, 1639–1644.
[34] J. N. Miller, J. C. Miller, *Statistics and Chemometrics for Analytical Chemistry*, Pearson Education Ltd., Harlow, **2005**.
[35] P. H. Rieger, in *Electrochemistry, 2nd ed.*, Springer Science & Business Media, Dordrecht, **2012**, p. 25.
[36] J. Stradins, B. Hasanli, *J. Electroanal. Chem.* **1993**, *353*, 57–69.

Received: September 9, 2017
Accepted: October 13, 2017
Published online on October 24, 2017

8. APPENDIX III

Electrochemical microcell based on silver solid amalgam electrode for voltammetric determination of pesticide difenzoquat

Gajdár Július, Barek Jiří, Fischer Jan

Sensors and Actuators B: Chemical

Year 2019, Volume 299, Article 126931

Sensors & Actuators: B. Chemical 299 (2019) 126931

Contents lists available at ScienceDirect

Sensors and Actuators B: Chemical

journal homepage: www.elsevier.com/locate/snb

Electrochemical microcell based on silver solid amalgam electrode for voltammetric determination of pesticide difenzoquat

Július Gajdár, Jiří Barek, Jan Fischer*

Charles University, Faculty of Science, Department of Analytical Chemistry, UNESCO Laboratory of Environmental Electrochemistry, Albertov 6, 12843 Prague 2, Czech Republic

ARTICLE INFO

Keywords:
Silver solid amalgam electrode
Voltammetry
Herbicide
Single drop analysis
Microcell

ABSTRACT

This study presents an application of a non-toxic mercury meniscus modified silver solid amalgam electrode as a reliable, user-friendly and sensitive sensor for the determination of herbicide difenzoquat as a model pollutant in micro volumes of samples. Difenzoquat gave one cathodic peak at around –1.4 V (vs. Ag/AgCl/3 mol L^{-1} KCl reference electrode) independent on pH (in the range 8–12). Sharp maxima greatly influenced the peak of the analyte and they were eliminated by the addition of gelatine as a surface-active compound. The optimal supporting electrolyte was found to be Britton-Robinson (BR) buffer with pH 12. Determination of the analyte in the 10 µL volume was carried out in a newly developed simple microcell with the amalgam working electrode. A procedure for fast and reliable removal of dissolved oxygen was used. Difenzoquat was therefore successfully determined by differential pulse voltammetry in BR buffer pH 12 and in model river water samples with addition of gelatine with limits of quantification 0.41 and 0.45 µmol L^{-1}, respectively. It was proved that this sensor can be directly used for monitoring of pollutants in volumes of tens of microliters of various samples with similar parameters as the determination in larger volumes.

1. Introduction

Monitoring of environmental pollutants is an important task of modern analytical chemistry. Their positive effects in the agriculture are often offset by their toxicity, carcinogenicity or mutagenicity and therefore, it is necessary to monitor their content in environmental samples of various sizes or volumes. Electrochemical methods are frequently used for the determination of pesticides because of their sensitivity, selectivity, and simple instrumentation [1,2]. They can be easily miniaturized and electrochemical sensors can be used for monitoring of pollutants. Several simple microcells have been developed and used for sample volumes in microliter and even submicroliter range. Two basic configurations used in batch arrangements can be divided according to the position of the working electrode [3]. In this work, an inverted state of the working electrode is used, mainly because it offers simple application of very small volumes on the surface of the electrode. The used microcell is modified from our previous publications with glassy carbon electrode [4,5]. Additionally, significant improvements have been made especially regarding removal of oxygen and overall sample manipulation.

Mercury is the best electrode material for the determination of reducible organic substances. However, because of the fear of its toxicity the use of mercury in electrochemical laboratories is decreasing [6]. This has led to the development of a new class of sensors based on non-toxic amalgams which share the wide cathodic potential window with mercury electrodes [7]. Moreover, they are more mechanically stable, and thus suitable for the development of new sensors and biosensors, for field-deployable portable devices, or for their use as detectors in flowing systems [8–10]. This type of sensor has been successfully used for voltammetric determinations of various organic compounds, e.g. insecticides [11,12], herbicides [13,14], environmental pollutants [15], and precursors of drugs [16]. Another type of novel mercury-based electrode is renewable silver-amalgam film electrode introduced in [17] which was recently used for determination of pesticides [18] and drugs [19,20]. Microcells designed for the determination of electrochemically active compounds in very small sample volumes have been based on hanging mercury drop [21], static mercury drop [22], mercury drop [23], amalgam-based [24] electrodes, combination of agar membrane with amalgam electrode [25], and multisensor design with various working electrodes [26].

Difenzoquat (DFQ, Scheme 1) is used as a herbicide and it is usually distributed as a 1,2-dimethyl-3,5-diphenyl-pyrazolium methyl sulphate [27]. This compound has been studied by electrochemical methods exclusively on mercury electrodes [28–31] using mixed or organic

* Corresponding author.
E-mail address: jfischer@natur.cuni.cz (J. Fischer).

https://doi.org/10.1016/j.snb.2019.126931
Received 19 November 2018; Received in revised form 8 April 2019; Accepted 31 July 2019
Available online 04 August 2019

solvents. In purely aqueous media DFQ had unfavourable adsorptive characteristics resulting in a non-linear concentration dependence [28]. DFQ can be determined by voltammetric methods because of a two-step, two-electron reduction of > C=N$^+$ < bond in its pyrazolium moiety [2,28,29] that is occurring at potentials more negative than −1 V. Only one study was dedicated to voltammetric determination of DFQ with the limit of detection 3.2 μmol L^{-1} by HPLC with voltammetric detection [31]. Another publication investigated adsorptive voltammetry of DFQ and concentrations in the order of nmol L^{-1} were detected [30].

The aim of this work is to develop a voltammetric method for the determination of DFQ at a mercury meniscus modified silver solid amalgam electrode (m-AgSAE) in a microcell for aqueous samples and to validate this method by determining DFQ in micro volumes of river water. This work also expands the usability of amalgam sensors by investigating electrochemical reduction of > C=N$^+$ < bond.

2. Experimental

2.1. Chemicals and reagents

A stock solution of DFQ (1 mmol L^{-1}, 1,2-dimethyl-3,5-diphenylpyrazolium methyl sulphate, CAS number: 43222-48-6, 99.9% from Sigma Aldrich, Germany) was prepared by dissolving 3.60 mg of the substance in 10 mL of deionized water and it was reported to be stable in aqueous solutions [27]. Two parts of Britton-Robinson (BR) buffer were prepared as follows: the acidic part consisted of mixture of 0.04 mol L^{-1} phosphoric, acetic, and boric acid, and alkaline part contained 1 mol L^{-1} sodium hydroxide (all p.a., Lach-ner, Czech Republic). BR buffers of given pH were prepared by mixing acidic and alkaline part. Phosphate buffer for determination in river water was prepared from 0.1 mol L^{-1} sodium hydrogen phosphate and sodium phosphate (both p.a., Lach-ner, Czech Republic) adjusted to pH 12 with 1 mol L^{-1} sodium hydroxide. All prepared solutions were stored in glass vessels in the dark at the laboratory temperature. Millipore Milli-Q system (Millipore, USA) was used for a production of deionized water.

2.2. Apparatus

Measurements were carried out with Eco-Tribo Polarograph controlled by Polar Pro 5.1 software (both Polaro-Sensors, Czech Republic) using a three-electrode system. A working mercury meniscus modified silver solid amalgam electrode (m-AgSAE, 0.5 mm diameter, Eco-Trend Plus, Czech Republic), Ag|AgCl|3 mol L^{-1} KCl reference electrode (RE, Elektrochemicke detektory, Turnov, Czech Republic) and a platinum wire auxiliary electrode (AUX, 0.4 mm diameter) were used. pH measurements were conducted with pH-meter Jenway 3510 with Jenway combined glass electrode type 924 005 (Bibby Scientific Ltd, United Kingdom). All voltammetric curves were measured at least 5 times at the laboratory temperature. DP voltammetric measurements were carried out with pulse amplitude −50 mV, pulse width of 100 ms, including 20 ms sampling time.

The DPV peak height was evaluated from the line connecting minima before and after the peak. Calculated parameters of calibration dependencies were evaluated with Origin software (OriginLab Corp., USA). Limits of quantification (*LOQ*) were calculated as a concentration corresponding to a tenfold of a standard deviation of ten subsequent measurements at the lowest measurable concentration. Linear dynamic ranges for calibration dependencies were calculated for confidence level 0.95 [32]. Voltammograms in figures are presented without any smoothing or other signal processing to keep information about the noise level.

2.3. Pre-treatment of m-AgSAE

Working m-AgSAE was pre-treated as described in [33]. The first procedure called amalgamation, or renewal of mercury meniscus consists of dipping the freshly mechanically polished electrode into a small volume of mercury for about 10 s. This was repeated about once a week or when the performance of the electrode rapidly deteriorated. The second procedure is activation and it was repeated before every series of measurements or as necessary. It consists of applying potential –2.2 V to the electrode for 300 s in a solution of 0.2 mol L^{-1} KCl in the presence of oxygen.

2.4. Procedures for the determination in 10 mL volume of the sample

Samples for voltammetric measurements in 10 mL were prepared by measuring an appropriate amount of the stock solution of DFQ into a 10.0 mL volumetric flask, two drops of 0.5% gelatine (Lachema, Brno) solution were then added (if not stated otherwise) and volumetric flask was filled with BR buffer pH 12.0 to the mark. Afterwards, the solution was transferred to the voltammetric cell, the whole solution was purged for 5 min with nitrogen and corresponding voltammograms were recorded.

River water samples were collected from Vltava River in Prague, Czech Republic. River water was at first filtered through the filtration paper. 9 mL of the river water sample spiked with a stock DFQ solution was transferred into a 10.0 mL volumetric flask, 2 drops of 0.5% gelatine solution were added, and filled with phosphate buffer (pH 12) to the mark.

2.5. Procedures for determination in 10 μL volume of the sample in the microcell

The microcell (Fig. 1) was slightly improved from our previous publications [4,5].Two drops of 0.5% gelatine were added to a 10.0 mL volumetric flask and it was filled to the mark with BR buffer (pH 12.0). Samples with DFQ were prepared by mixing appropriate amounts of the prepared BR buffer (pH 12.0) with gelatine and the stock solution of the analyte to the final volume of 1.0 mL into a vial. Afterwards, the prepared solution was purged with nitrogen for 5 min. Nitrogen was at first saturated with water vapours to minimize the evaporation of the sample drop. A moveable plastic tube prepared by cutting 1 mL pipette tip was used to enclose the whole microcell and to achieve nitrogen atmosphere inside. All electrodes were fixed by holders before the series of measurements and it was not necessary to move them until activation of the working electrode was necessary. Before the application of a new drop the space between electrodes was washed with a few drops of deionized water, which were then carefully dried with cotton swabs. The microcell was then enclosed by the plastic tube and it was left on its own for about 1 min to create nitrogen atmosphere inside. 10 μL of the sample was then transferred to the microcell in-between the reference electrode and the working electrode via the Hamilton syringe through a small hole in the tube and 5 consequent measurements were performed immediately after the application of the drop. During that time another sample was transferred to the vial and purged with nitrogen for 5 min.

Model river water samples were prepared as follows: two drops of 0.5% gelatine were filled to the mark with phosphate buffer pH 12.0 in a 10.0 mL volumetric flask. Samples with DFQ were prepared by mixing 0.9 mL of river water spiked with the stock DFQ solution with the solution of phosphate buffer and gelatine to the final volume 1.0 mL into a vial followed by the same procedure as described above.

3. Results and discussion

3.1. Electrochemistry of difenzoquat

At first, the dependence of voltammetric behaviour of DFQ on pH was investigated. DFQ gave several peaks in BR buffer media. The reduction of DFQ was not observable at pH lower than 8 in the studied range of pH 2–12. In the pH range of 8–12, only the first peak was

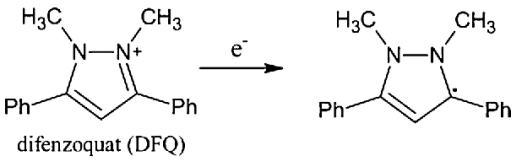

Scheme 1. Mechanism of DFQ reduction (adapted from [28,29]).

evaluated, and its potential was constant at –1.33 V (Fig. 2).

Sharp unrepeatable maxima that were observed after the first peak were eliminated by the addition of gelatine into the measured solution which is routinely used to eliminate similar maxima in polarography [34]. The comparison of DC voltammograms (Fig. 3) illustrates this phenomenon. The negative half-wave potential shift (around −60 mV) to –1.39 V can be attributed to gelatine covering the electrode surface thus making the reduction of DFQ more difficult. No significant change of the current response was observed after the addition of gelatine. The amount of gelatine added was not optimized; however, no change in the peak position or its height was observed between different measurements with the addition of 2 drops (around 100 µL) of gelatine to the final concentration around 50 µg mL^{-1}.

The dependence on pH suggests that there are no protons involved in the reduction of DFQ at alkaline pH. Investigation by cyclic voltammetry at pH 12 confirmed only one cathodic irreversible peak in the presence of gelatine with no peaks in the reverse scan. CV without gelatine gives several maxima after the first voltammetric peak as observed by DPV. These observations are in accordance with a first step of mechanism proposed in [28] and it could suggest one electron reduction of $>C=N^+<$ group to a radical according to the Scheme 1 (adapted from [28,29]). The second step proposed in [28] is one electron and one proton reduction, however, as described earlier, no protons are involved in the reduction in this case. The radical then can also presumably react with another radical and form a dimer as the final product.

The peak current response was practically the same in the pH range 10-12. More alkaline pH 12 with the broadest potential window proved to be optimal as the hydrogen evolution was less interfering with the peak evaluation even at the lowest concentrations. Subsequent measurements in the BR buffer (pH 12.0) with the addition of gelatine on the freshly activated electrode provided very good reproducibility (c = 0.1 mmol L^{-1}, N = 20, RSD = 3%) and no passivation of the electrode surface was observed.

3.2. Determination in 10 mL samples

For the sake of comparison, the effect of gelatine on the calibration dependency was studied. DFQ was firstly determined in the BR buffer

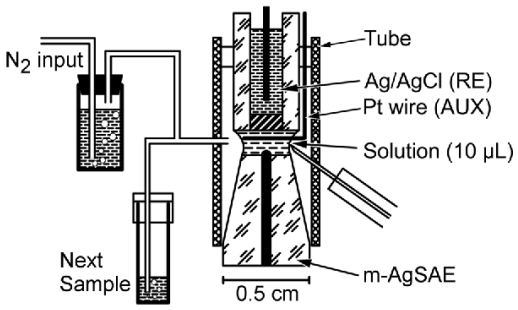

Fig. 1. Simplified scheme of the microcell used for measurements of 10 µL samples with the removal of oxygen using a working m-AgSAE, a reference Ag|AgCl|3 mol L^{-1} KCl electrode (RE) and a platinum wire auxiliary electrode (AUX).

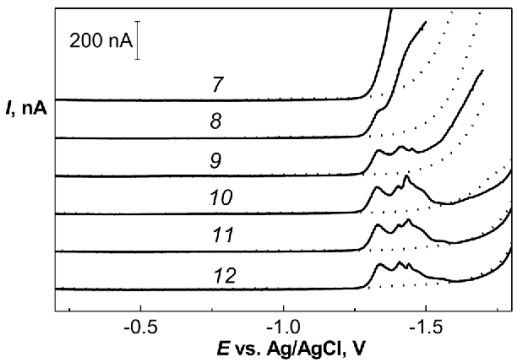

Fig. 2. DP voltammograms of DFQ (c = 0.1 mmol L^{-1}) at m-AgSAE in BR buffer with different pH given above voltammogram without gelatine. Dotted curves represent supporting electrolyte solutions.

(pH 12) without the addition of gelatine. Sharp maxima were eliminated at lower micromolar concentrations to only one peak; however, the peak height did not give a linear dependency on the concentration of DFQ. This has led to the conclusion that determination without the addition of gelatine is unsatisfactory and this observation is in agreement with previous findings at mercury electrodes [28].

DFQ was therefore determined in the BR buffer (pH 12) with the addition of two drops of 0.5% gelatine solution. In this case DFQ gave one single peak that was shifting from –1.50 V to –1.40 V with the increasing concentration. This effect is related to the presence of gelatine in the solution as it was not observed in the absence of gelatine. Observed calibration dependence had to be divided into two linear ranges as seen in Table 1. Linearity of both ranges was calculated for the confidence level 0.95. The slope and the intercept of the calibration curve have significantly changed at higher concentration range (4–100 µmol L^{-1}) probably because of the complete coverage of the electrode surface by DFQ. This phenomenon is frequently observed in voltammetric determinations at solid electrodes.

Practical application of the developed method was tested with model samples of river water spiked with DFQ. More concentrated 0.2 M buffer with a higher buffer capacity had to be used to achieve very alkaline pH 12.0 in the prepared river water sample. Phosphate buffer was used instead of BR buffer to simplify the preparation. The developed method provided good figures of merits for the

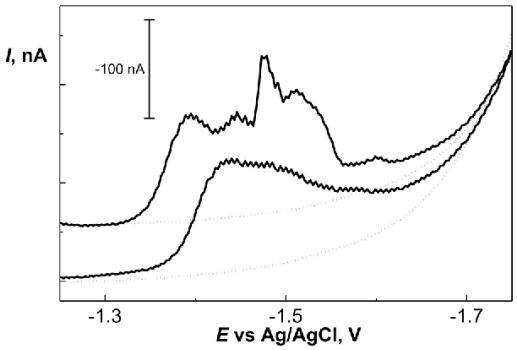

Fig. 3. DC voltammograms (20 mV s^{-1}) of DFQ (c = 0.1 mmol L^{-1}) in BR buffer pH 12 at m-AgSAE without gelatine (upper solid curve) and in the presence of 50 µg mL^{-1} gelatine (lower solid curve). Supporting electrolyte is depicted as dotted line under the respective curve. Curves were offset in the direction of y-axis.

determination of DFQ in river water with *LOQ* 0.45 μmol L^{-1}, comparable to *LOQ* 0.40 μmol L^{-1} in BR buffer. The calibration dependency had to be divided into two linear sections again with significantly lower slope at higher concentration range.

3.3. Determination in 10 μL samples

Parameters of methods and media used and optimized for 10 mL volume were duplicated for the work in a single drop of a solution for the sake of comparison of results obtained with different sample volumes. Volume 10 μL was chosen as optimal for this type of microcell. Higher volumes (20 μL and more) were oversized for this microcell and lower volumes (5 μL and less) would make an application of a sample and creating a contact between two electrodes much more difficult. The distance between the electrodes was fixed only by position of holders and was kept at approximately 2 mm. Variation in the distance (and volume accordingly) between 1–3 mm had no influence on the peak height; however, the distance shorter than 1 mm gave lower peak height. This proves that small variations in the microcell assembly have no effect on the voltammetric signal.

One of the issues that arise while determining compounds by cathodic voltammetry is a negative influence of oxygen that provides two large signals (oxygen and then hydrogen peroxide reduction) in the supporting electrolyte that interferes with the determination of any reducible substance. In our previous publications [4,5] oxygen was removed in nitrogen atmosphere, however this process was time-consuming; it took around 10–20 min for nitrogen to displace oxygen from the solution. Improvement in this case was made by purging the sample solution before its application into the microcell. It makes the whole oxygen removal procedure much faster because while one sample was measured, next sample was being purged with nitrogen and it was ready to be transferred to the microcell without any downtime or waiting required. For one measurement of 10 μL sample the overall volume of sample must be about 2 to 3-times the necessary volume (in this case ~20 to 30 μL) to account for loses contributed to the sample handling process. Oxygen removal with smaller samples should be performed directly in the microcell as in our previous publications [4,5] which is, however, more time consuming. Transfer from the vial had to be made with a Hamilton syringe into the enclosed microcell filled with nitrogen. Transfer with an automatic pipette or transfer to the open microcell renders the whole purging worthless as the oxygen returns to the solution.

Reproducibility of subsequent measurements in BR buffer (pH 12.0) with the addition of gelatine on the freshly activated electrode provided very good results comparable to 10 mL of a solution (c = 0.1 mmol L^{-1}, N = 20, RSD = 4%) without any apparent trends. Calibration dependencies in a drop of a solution had similar parameters as dependencies obtained in 10 mL. The whole measured range was similarly divided into two linear ranges (Table 1) and also a shift of the peak potential was observed. Presumably it was caused by the same reasons as in 10 mL volume that are unrelated to the miniaturization of the voltammetric method. Limits of quantification 0.41 and 0.45 μmol L^{-1} for deionized water and river water, respectively, were almost equal to values obtained in 10 mL of a solution. This comparison of the concentration dependency in a single drop of a solution (10 μL) and 10 mL is also illustrated in Fig. 4 for the determination in a river water sample.

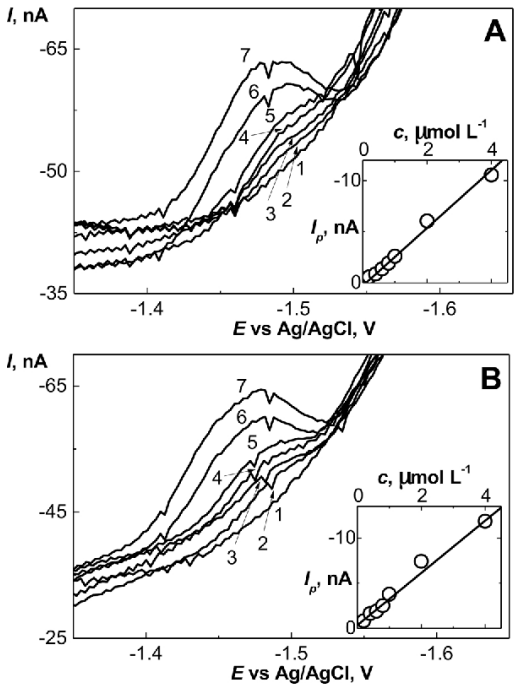

Fig. 4. DP voltammograms of DFQ (0.00 (1); 0.40 (2); 0.60 (3); 0.80 (4); 1.00 (5); 2.00 (6); and 4.00 (7) μmol L^{-1}) in 10 mL volume (**A**) and in a drop of a solution (10 μL volume) (**B**) obtained at m-AgSAE. Spiked river water – phosphate buffer (pH 12) (9:1) mixture in the presence of gelatine (50 μg mL^{-1}) was analysed. The calibration linear curve is in the inset.

Table 1
Calibration straight line parameters for DPV determination of DFQ at m-AgSAE in various matrices and volumes using buffers with pH 12.0 as supporting electrolytes and gelatine (50 μg mL^{-1}) to suppress observed maxima.

Volume	Medium	c, μmol L^{-1}	Slope, mA L mol^{-1}	Intercept, nA	Corr. coefficient	*LOQ*, μmol L^{-1}
10 mL	Deionised water	4–100	−2.247 ± 0.031	−16.98 ± 0.55	−0.9993	–
		0.2–4	−6.33 ± 0.29	−0.18 ± 0.26[a]	−0.9949	0.40
	River water	4–100	−0.954 ± 0.016	−7.00 ± 0.34	−0.9990	–
		0.2–4	−2.81 ± 0.16	+0.29 ± 0.13	−0.9924	0.45
10 μL	Deionised water	4–100	−1.450 ± 0.029	−11.24 ± 0.44	−0.9986	–
		0.2–4	−4.13 ± 0.16	−0.58 ± 0.24	−0.9962	0.41
	River water	4–100	−1.019 ± 0.027	−8.01 ± 0.35	−0.9976	–
		0.2–4	−2.83 ± 0.14	−0.65 ± 0.35	−0.9942	0.45

[a] Intercept is not statistically different from zero.

4. Conclusion

The proposed miniaturized voltammetric cell based on m-AgSAE was successfully applied for DP voltammetric determination of herbicide difenzoquat in samples with volume of 10 µL. The compound gave one cathodic peak (independent of pH) at very negative potentials around –1.39 V. This reduction was observable thanks to one of the advantages of silver solid amalgam electrodes - their wide cathodic potential window, wider than any other non-mercury-based electrode material. The optimal supporting electrolyte was found to be BR buffer pH 12 especially because it offered the widest potential window and easiest evaluation. The addition of gelatine eliminated sharp maxima after the reduction wave. It also seems to eliminate the problem with the non-linear concentration dependence in aqueous solutions that was the problem in earlier publications [28,29]. The analyte was then successfully determined by DPV in BR buffer (pH 12) and in spiked river water samples with phosphate buffer (pH 12). Calibration dependencies had two linear ranges with lower slope at higher concentrations. Limits of quantification around 0.4 µmol L^{-1} were achieved in both deionized and river water samples. *LOQs* achieved in microcell were practically the same as *LOQs* achieved by standard voltammetric procedure with 10 mL sample.

Therefore, it was proved that proposed microcell offers the same sensitivity for sensing DFQ with several orders lower chemicals consumption and sample volume. This microcell also offers a simple and fast way for work with samples of 10 µL volume for the determination of any reducible electrochemical species, because of procedures designed to get rid of dissolved oxygen from samples in a very convenient and simple way. Moreover, small sample volume is required in the case of preliminary separation and preconcentration when the dilution of extract and/or residue after evaporation to 10 ml would increase *LOD* one thousand times as compared with the dilution to the final volume of 10 µL.

Acknowledgement

This research was supported by the Czech Science Foundation (project 17-03868S).

References

[1] J. Barek, J. Fischer, T. Navrátil, K. Pecková, B. Yosypchuk, J. Zima, Nontraditional electrode materials in environmental analysis of biologically active organic compounds, Electroanalysis 19 (2007) 2003–2014, https://doi.org/10.1002/elan.200703918.
[2] J. Fischer, H. Dejmkova, J. Barek, Electrochemistry of pesticides and its analytical applications, Curr. Org. Chem. 15 (2011) 2923–2935, https://doi.org/10.2174/138527211798357146.
[3] Y.I. Tur'yan, Microcells for voltammetry and stripping voltammetry, Talanta 44 (1997) 1–13, https://doi.org/10.1016/S0039-9140(96)02040-1.
[4] J. Gajdár, T. Goněc, J. Jampílek, M. Brázdová, Z. Bábková, M. Fojta, J. Barek, J. Fischer, Voltammetry of a novel antimycobacterial agent 1-hydroxy-N-(4-nitrophenyl)naphthalene-2-carboxamide in a single drop of a solution, Electroanalysis 30 (2018) 38–47, https://doi.org/10.1002/elan.201700547.
[5] J. Gajdár, J. Barek, M. Fojta, J. Fischer, Micro volume voltammetric determination of 4-nitrophenol in dimethyl sulfoxide at a glassy carbon electrode, Mon. Chem. 148 (2017) 1639–1644, https://doi.org/10.1007/s00706-017-1954-4.
[6] J. Gajdar, E. Horakova, J. Barek, J. Fischer, V. Vyskocil, Recent applications of mercury electrodes for monitoring of pesticides: a critical review, Electroanalysis 28 (2016) 2659–2671, https://doi.org/10.1002/elan.201600239.
[7] L. Novotny, B. Yosypchuk, Solid silver amalgam electrodes, Chem. Listy 94 (2000) 1118–1120.
[8] B. Yosypchuk, L. Novotný, Electrodes of nontoxic solid amalgams for electrochemical measurements, Electroanalysis 14 (2002) 1733–1738, https://doi.org/10.1002/elan.200290018.
[9] A. Danhel, B. Josypcuk, J. Barek, M. Fojta, Possibilities and prospects of silver amalgam in electroanalytical chemistry, Chem. Listy 110 (2016) 215–221.
[10] B. Yosypchuk, J. Barek, Properties of solid and paste amalgam electrodes different from metal mercury electrodes, Chem. Listy 103 (2009) 284–290.
[11] P. Chorti, J. Fischer, V. Vyskocil, A. Economou, J. Barek, Voltammetric determination of insecticide thiamethoxam on silver solid amalgam electrode, Electrochim. Acta 140 (2014) 5–10, https://doi.org/10.1016/j.electacta.2014.01.081.
[12] K. Novakova, V. Hrdlicka, T. Navratil, M. Harvila, J. Zima, J. Barek, Application of silver solid amalgam electrode for determination of formamidine amitraz, Mon. Chem. 147 (2016) 181–189, https://doi.org/10.1007/s00706-015-1575-8.
[13] L. Janikova, R. Selesovska, M. Rogozinska, M. Tomaskova, J. Chylkova, Sensitive voltammetric method for determination of herbicide metribuzin using silver solid amalgam electrode, Mon. Chem. 147 (2016) 219–229, https://doi.org/10.1007/s00706-015-1555-z.
[14] L. Janikova-Bandzuchova, R. Selesovska, J. Chylkova, V. Nesnidalova, Voltammetric analysis of herbicide picloram on the silver solid amalgam electrode, Anal. Lett. 49 (2016) 19–36, https://doi.org/10.1080/00032719.2014.979294.
[15] A. Hajkova, J. Hranicek, J. Barek, V. Vyskocil, Voltammetric determination of trace amounts of 2-aminofluoren-9-one at a mercury meniscus modified silver solid amalgam electrode, Electroanalysis 25 (2013) 295–302, https://doi.org/10.1002/elan.201200408.
[16] Š. Skalová, T. Navrátil, J. Barek, V. Vyskočil, Voltammetric determination of sodium anthraquinone-2-sulfonate using silver solid amalgam electrodes, Mon. Chem. 148 (2017) 577–583, https://doi.org/10.1007/s00706-017-1926-8.
[17] B. Bas, Refreshable mercury film silver based electrode for determination of chromium(VI) using catalytic adsorptive stripping voltammetry, Anal. Chim. Acta 570 (2006) 195–201, https://doi.org/10.1016/j.aca.2006.04.013.
[18] M. Brycht, S. Skrzypek, V. Guzsvany, J. Berenji, Conditioning of renewable silver amalgam film electrode for the characterization of clothianidin and its determination in selected samples by adsorptive square-wave voltammetry, Talanta 117 (2013) 242–249, https://doi.org/10.1016/j.talanta.2013.08.048.
[19] O. Vajdle, V. Guzsvany, D. Skoric, J. Anojcic, P. Jovanov, M. Avramov-Ivic, J. Csanadi, Z. Konya, S. Petrovic, A. Bobrowski, Voltammetric behavior of erythromycin ethylsuccinate at a renewable silver-amalgam film electrode and its determination in urine and in a pharmaceutical preparation, Electrochim. Acta 191 (2016) 44–54, https://doi.org/10.1016/j.electacta.2015.12.207.
[20] O. Vajdle, V. Guzsvany, D. Skoric, J. Csanadi, M. Petkovic, M. Avramov-Ivic, Z. Konya, S. Petrovic, A. Bobrowski, Voltammetric behavior and determination of the macrolide antibiotics azithromycin, clarithromycin and roxithromycin at a renewable silver – amalgam film electrode, Electrochim. Acta 229 (2017) 334–344, https://doi.org/10.1016/j.electacta.2017.01.146.
[21] W.L. Underkofler, I. Shain, Microcell for voltammetry with the hanging mercury drop electrode, Anal. Chem. 33 (1961) 1966–1967, https://doi.org/10.1021/ac50154a064.
[22] C.N. Yarnitzky, Second-generation automated voltammetric cell, Electroanalysis 2 (1990) 581–585, https://doi.org/10.1002/elan.1140020803.
[23] L. Huderová, K. Štulík, A contribution to the problem of increasing the sensitivity of anodic-stripping voltammetry, Talanta 19 (1972) 1285–1293, https://doi.org/10.1016/0039-9140(72)80125-5.
[24] A. Hájková, V. Vyskočil, B. Josypčuk, J. Barek, A miniaturized electrode system for voltammetric determination of electrochemically reducible environmental pollutants, Sens. Actuator B Chem. 227 (2016) 263–270, https://doi.org/10.1016/j.snb.2015.11.136.
[25] Š. Skalová, L.M. Gonçalves, T. Navrátil, J. Barek, J.A. Rodrigues, V. Vyskočil, Miniaturized voltammetric cell for cathodic voltammetry making use of an agar membrane, J. Electroanal. Chem. 821 (2018) 47–52, https://doi.org/10.1016/j.jelechem.2017.12.073.
[26] T. Navratil, B. Yosypchuk, J. Barek, A multisensor for electrochemical sequential autonomous automatic measurements, Chem. Anal. Warsaw 54 (2009) 3–17.
[27] W.W. Donald, Difenzoquat, in: W.W. Donald (Ed.), Systems of Weed Control in Wheat in North America, Weed Science Society of America, Champaign, Illinois, 1990, pp. 298–320.
[28] L. Pospíšil, M.P. Colombini, R. Fuoco, V.V. Strelets, Electrochemical properties of difenzoquat herbicide (1,2-dimethyl-3,5-diphenyl-pyrazolium), J. Electroanal. Chem. Interfacial Electrochem. 310 (1991) 169–178, https://doi.org/10.1016/0022-0728(91)85260-V.
[29] L. Pospíšil, J. Hanzlík, R. Fuoco, M.P. Colombini, Electrochemical and spectral evidence of the inclusion of the herbicide difenzoquat by cyclodextrins in aqueous solution, J. Electroanal. Chem. 368 (1994) 149–154, https://doi.org/10.1016/0022-0728(93)03109-3.
[30] L. Pospíšil, J. Hanzlík, R. Fuoco, N. Fanelli, Growth of compact layers at the interface: part VI. Adsorption properties of difenzoquat herbicide (1,2-dimethyl-3,5-diphenyl-pyrazolium), J. Electroanal. Chem. 334 (1992) 309–321, https://doi.org/10.1016/0022-0728(92)80580-W.
[31] I. Rühling, H. Schäfer, W. Ternes, HPLC online reductive scanning voltammetric detection of diquat, paraquat and difenzoquat with mercury electrodes, Fresenius J. Anal. Chem. 364 (1999) 565–569, https://doi.org/10.1007/s002160051387.
[32] J.N. Miller, J.C. Miller, Statistics and Chemometrics for Analytical Chemistry, Pearson Education Ltd., Harlow, 2005.
[33] B. Yosypchuk, J. Barek, Analytical applications of solid and paste amalgam

electrodes, Crit. Rev. Anal. Chem. 39 (2009) 189–203, https://doi.org/10.1080/10408340903011838.
[34] J. Heyrovský, P. Zuman, Practical Polarography: An Introduction for Chemistry Students, Academic Press, London, 1968, pp. 162–172.

Július Gajdár is pursuing PhD degree under the supervision of Prof. Jiří Barek at the Charles University (Czech Republic), Faculty of Science, Department of Analytical Chemistry. His research interests include electroanalytical chemistry of various organic compounds, pesticides and pharmaceuticals on novel electrode materials with focus on miniaturization of applied methods.

Jiří Barek is a professor at the Charles University (Czech Republic), Faculty of Science, Department of Analytical Chemistry, and the Head of the UNESCO Laboratory of Environmental Electrochemistry. He published more than 400 papers (h-index of 36). His main research interest is the development of new voltammetric and amperometric methods for detection of trace amounts of biologically active organic compounds important from the point of view of the protection of the environment and human health.

Jan Fischer is an assistant professor at the Charles University (Czech Republic), Faculty of Science, Department of Analytical Chemistry. His current research is focused on application of modern electrode materials, mainly those based on silver amalgam, for voltammetric and amperometric determination of bioactive organic compounds.

9. APPENDIX IV

Electrochemistry of ring-substituted 1-hydroxynaphthalene-2-carboxanilides: Relation to structure and biological activity

Gajdár Július, Tsami Konstantina, Michnová Hana, Goněc Tomáš, Brázdová Marie, Soldánová Zuzana, Fojta Miroslav, Jampílek Josef, Barek Jiří, Fischer Jan

Electrochimica Acta

Year 2019, submitted

Elsevier Editorial System(tm) for
Electrochimica Acta

Manuscript Draft

Manuscript Number:

Title: Electrochemistry of ring-substituted 1-hydroxynaphthalene-2-carboxanilides: Relation to structure and biological activity

Article Type: Research Paper

Keywords: Hydroxynaphthalene-2-carboxanilides; Antimycobacterial activity; Photosynthetic electron transport inhibition; Hammett correlation; Structure-activity relationship

Corresponding Author: Dr. Jan Fischer, Ph.D.

Corresponding Author's Institution: Charles University in Prague, Faculty of Science

First Author: Július Gajdár

Order of Authors: Július Gajdár; Konstantina Tsami; Hana Michnová; Tomáš Goněc, Dr.; Marie Brázdová, Dr.; Zuzana Soldánová; Miroslav Fojta, Assoc. Prof.; Josef Jampílek, Prof.; Jiří Barek, Prof.; Jan Fischer, Dr.

Abstract: Twenty-two novel antimycobacterial agents, 1-hydroxynaphthalene-2-carboxanilides, were studied by cyclic voltammetry on a glassy carbon electrode in a phosphate buffer pH 7.2 - dimethyl sulfoxide mixed medium (9:1; v/v). All compounds exhibited similar voltammetric behavior with one irreversible anodic signal in the range 100-300 mV corresponding to the oxidation of hydroxyl group on the naphthalene moiety. A shift of the oxidation potential was caused solely by electron donating or withdrawing effects of substituents and their position on the benzene moiety. Mechanism of oxidation in the studied medium was briefly outlined. Values of oxidation potentials exhibited very good linear correlation with calculated Hammett σ substituent constants. For all active compounds, a relationship between oxidation potentials and MIC or IC50 values obtained from in vitro screening was investigated in detail. Primary in vitro screening of synthesized compounds was previously performed against three species of Mycobacterium pathogens. Additionally, their activity related to the inhibition of photosynthetic electron transport (PET) in spinach chloroplasts was tested in previous publications. In vitro screening against Mycobacterium tuberculosis was performed here for the first time with 1-hydroxy-N-(3-trifluoromethylphenyl)naphthalene-2-carboxamide being the most effective (MIC = 11.7 μmol L−1). Furthermore, several other compounds showed higher antimycobacterial activity than the standard isoniazid. Relation of biological activities and oxidation potentials was successfully found in some cases; however, final correlations must also be considered with other physical and chemical factors contributing to the biological activity. Relation of structure, biological activity and electrochemical potential was also studied by cyclic voltammetry in cathodic area for three compounds containing reducible nitro moiety.

Electrochemistry of ring-substituted 1-hydroxynaphthalene-2-carboxanilides: Relation to structure and biological activity

Július Gajdár [1], Konstantina Tsami [2], Hana Michnová [3], Tomáš Goněc [4], Marie Brázdová [5], Zuzana Soldánová [5], Miroslav Fojta [5], Josef Jampílek [3,6], Jiří Barek [1], and Jan Fischer [1]

[1] Charles University, Faculty of Science, Department of Analytical Chemistry, UNESCO Laboratory of Environmental Electrochemistry, Albertov 6, Prague 2, 12843, Czech Republic

[2] National and Kapodistrian University of Athens, Department of Chemistry, Laboratory of Analytical Chemistry, Athens, 15771, Greece

[3] Palacký University, Faculty of Science, Regional Centre of Advanced Technologies and Materials, Šlechtitelů 27, Olomouc, 78371, Czech Republic

[4] University of Veterinary and Pharmaceutical Sciences Brno, Faculty of Pharmacy, Department of Chemical Drugs, Palackého 1, Brno, 61242, Czech Republic

[5] Institute of Biophysics of the Czech Academy of Sciences, Královopolská 135, Brno, 61265, Czech Republic

[6] Comenius University, Faculty of Natural Sciences, Department of Analytical Chemistry, Ilkovičova 6, Bratislava, 84215, Slovakia

Abstract

Twenty-two novel antimycobacterial agents, 1-hydroxynaphthalene-2-carboxanilides, were studied by cyclic voltammetry on a glassy carbon electrode in a phosphate buffer pH 7.2 – dimethyl sulfoxide mixed medium (9:1; v/v). All compounds exhibited similar voltammetric behavior with one irreversible anodic signal in the range 100-300 mV corresponding to the oxidation of hydroxyl group on the naphthalene moiety. A shift of the oxidation potential was caused solely by electron donating or withdrawing effects of substituents and their position on the benzene moiety. Mechanism of oxidation in the studied medium was briefly outlined. Values of oxidation potentials exhibited very good linear correlation with calculated Hammett σ substituent constants. For all active compounds, a relationship between oxidation potentials and MIC or IC_{50} values obtained from *in vitro* screening was investigated in detail. Primary *in vitro* screening of synthesized compounds was previously performed against three species of *Mycobacterium* pathogens. Additionally, their activity related to the inhibition of photosynthetic electron transport (PET) in spinach chloroplasts was tested in previous publications. *In vitro* screening against *Mycobacterium tuberculosis* was performed here for the first time with 1-hydroxy-*N*-(3-trifluoromethylphenyl)naphthalene-2-carboxamide being the most effective (MIC = 11.7 μmol L^{-1}). Furthermore, several other compounds showed higher antimycobacterial activity than the standard isoniazid. Relation of biological activities and oxidation potentials was successfully found in some cases; however, final correlations must also be considered with other physical and chemical factors contributing to the

biological activity. Relation of structure, biological activity and electrochemical potential was also studied by cyclic voltammetry in cathodic area for three compounds containing reducible nitro moiety.

Keywords: Hydroxynaphthalene-2-carboxanilides, Antimycobacterial activity, Photosynthetic electron transport inhibition, Hammett correlation, Structure-activity relationship

1. Introduction

Tuberculosis (TB) is still one of the top ten causes of death worldwide and it is a leading cause of death caused by a single infectious agent; a pathogen called *Mycobacterium tuberculosis*. There were around 10 million new cases of TB in 2017 and approximately 0.6 million of them were caused by emerging multidrug-resistant strains of pathogens. Treatment in those cases by the most common first-line drugs used for treatment of TB, isoniazid and rifampicin, is ineffective. It complicates and prolongs the healing process and an individual therapy lasting several months is necessary [1]. All of these facts are the reason for rapid and intense research into novel molecular scaffolds [2]. Other nontuberculous *Mycobacteria* are also responsible for a broad spectrum of diseases and are especially dangerous for immunocompromised patients [3, 4].

Emergence of drug-resistant strains of *Mycobacterium tuberculosis* has led to the development of novel antimycobacterial agents based on the structure of hydroxynaphthalenecarboxanilide. These novel agents demonstrated spectrum of anti-infectious [5-12] and/or antiproliferative properties [13, 14]. These structurally simple compounds, regarded as the ring analogues of salicylanilides (e.g., niclosamide [7]) can be considered as privileged structures. Their activity depends on the mutual position of carboxamide and phenolic moieties [5-7, 9, 12], therefore analogues with various position of phenolic moiety show different spectrum of biological activities as well as potency. A carboxamide linker (CONH) mimicking a peptide bond is crucial for the activity, because by the means of this moiety, a compound is bound to their supposed targets. Following the polypharmacology idea, these compounds can be classified as multi-target compounds, since they are able to affect various target structures, especially in microbial pathogens, similarly as salicylanilides [15-18]. It is assumed that anilide part of the molecule is responsible for influencing the physicochemical properties and binding strength of the test compounds to the potential target. Moreover, variously substituted anilide rings cause an excess or lack of electrons in the amide bond (in connection with the nature of the substituent and its electron donating or withdrawing properties), which causes various acidity/oxidizability of a spatially close phenolic moiety, resulting in the wide spectrum of activity and potency of the individual compounds. These subtle changes in oxidizability can be presumably studied by electrochemical methods in which case a change of measured oxidation potential would be an indicator of different structure and, therefore, possibly also a different activity and potency.

This study concerns only one subgroup of these compounds, 1-hydroxynaphthalene-2-carboxanilides, that were prepared and tested by Gonec et al. [5]. It should be noted that this type of compounds is able to inhibit photosynthetic electron transport (PET) in spinach (*Spinacia oleracea* L.) chloroplasts. The formation of hydrogen bonds between the CONH moiety and the target proteins in photosynthetic centers of thylakoid membranes changes protein conformation resulting in PET inhibition. This amide moiety is present in many herbicides acting as PET inhibitors in photosystem (PS) II, where they cause displacement of plastoquinone (Q_B) from its binding pocket in one of the protein subunits of PS II, the D1 protein [15, 19]. It can be hypothesized that above-mentioned hydroxynaphthalenecarboxanilides are able to inhibit cell growth by the inhibition of the respiration by several possible targets/mechanisms of action, i.e. by the inhibition of ATP synthase or cytochrome bc1, or by the inhibition of the electron transport [4, 7, 9, 20-22]. Thus, it was observed that antimycobacterial activity correlates with PET inhibition profile [5-11, 15, 23-25].

A pilot electrochemical study of a model compound 1-hydroxy-*N*-(4-nitrophenyl) naphthalene-2-carboxamide was carried out by our team in very small sample volumes. This compound provided one anodic and one cathodic signal corresponding to the oxidation of hydroxyl group and reduction of nitro group, respectively. Mechanisms of redox processes were outlined and studied by cyclic voltammetry [26]. Findings included in that work were used as a baseline for this current study. Phenols are electrochemically oxidized to radicals which then undergo coupling reactions to create dimers or they can be further electrochemically oxidized (at more positive potentials) to form quinone-like structures [27-29]. Reducible nitro substituted aromatic compounds have been investigated extensively by electrochemical methods [27, 30-32].

This study aims to investigate the relationship between structure and electrochemical potential based on application of Hammett substituent constants that were at first collected by Zuman [33]. Investigation of salicylaldehyde anils [34] and some boron heterocycles [35] even reveals an effect of substituents that are connected to the oxidation center through more atoms and delocalized systems. The aim of this work is also to investigate relationship between electrochemistry and biological activity based on recent studies that have shown the correlation between electrochemical behavior, structure and biological activity for some groups of compounds [36-40]. Relations between electrochemical data, biological activity and biochemical mechanism of action of antibacterial agents, derivatives of quinoxalines di-*N*-oxides, was investigated [36, 41]. Another group of antibiotic compounds based on arylazoxy derivatives was studied and a correlation between Hammett σ substituent constant and electrochemical potential of reduction of studied compounds was proved [37]. However, it must be noted that biological processes are complex and thus an absolute correlation with electrochemistry cannot be expected and numbers of other parameters must be considered like lipophilicity, diffusion, solubility, metabolism, membrane permeability, absorption, active site binding, etc. [36, 38]. Alternatively, many biological processes are based on redox reactions and studying electron transfer mechanism of those reactions by electrochemical methods can be useful for observing and predicting biological phenomena [42, 43]. Correlation between

electrochemistry and biological activity can also point to bio-reduction (bio-oxidation) playing an important role in the mode of action [39, 40]. The prediction of substituent effect can even possibly aid designing more powerful derivatives [44].

2. Experimental

2.1. Chemicals

Compounds **1-8c** were synthetized according to methods described in detail in [5] and schematically depicted in Scheme 1.

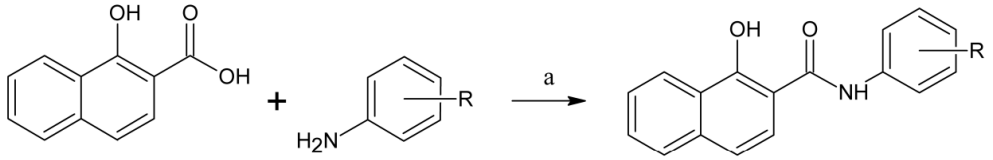

Scheme 1: Synthesis of ring-substituted 1-hydroxynaphthalene-2-carboxanilides **1-8c**: R = H (**1**), OCH_3 (**2a-c**), CH_3 (**3a-c**), F (**4a-c**), Cl (**5a-c**), Br (**6a-c**), CF_3 (**7a-c**), NO_2 (**8a-c**); (a) PCl_3, chlorobenzene, microwave (adapted from [5]).

2.2 Electrochemical procedures

Appropriate amount of solid compound **1-8c** was weighted and dissolved in 1 mL of DMSO (p.a., Penta, Czech Republic) to the concentration 1 mmol L^{-1}. 0.1 mol L^{-1} phosphate buffer was used as a supporting electrolyte and it was prepared by mixing disodium hydrogenphosphate and sodium dihydrogen phosphate adjusted to pH 7.2 by concentrated 1 mol L^{-1} sodium hydroxide solution (all p.a., Lach-ner, Czech Republic). Prepared solutions were stored in a fridge in the dark.

All voltammetric measurements were carried out on Eco-Tribo Polarograph controlled by Polar Pro 5.1 software (Polaro-Sensors, Czech Republic). A three-electrode system was used with a working glassy carbon disc electrode (GCE, 2 mm diameter, Metrohm, Switzerland), an Ag|AgCl|3 mol L^{-1} KCl reference electrode (Elektrochemicke detektory, Turnov, Czech Republic), and an auxiliary platinum wire electrode (0.5 mm diameter). pH was measured with pH-meter Jenway 3510 (Bibby Scientific Ltd, United Kingdom) with Jenway combined glass electrode (924 005) calibrated using standard aqueous buffers. The working GCE had to be pre-treated before every measurement by polishing to mirror-like appearance with an aqueous slurry of alumina powder (1.1 μm) on a polishing pad and then it was sonicated for 30s in methanol and for 30s in deionized water.

Cyclic voltammetry (CV) was usually carried out at a scan rate 50 mV s^{-1}. Daily variations of the reference electrode potential were resolved by evaluating the peak of 50 μmol L^{-1} $K_4[Fe^{II}(CN)_6]$ in the separate solution containing the same supporting electrolyte that was

measured in regular intervals. Measured potentials are usually reported after subtraction of $[Fe^{II}(CN)_6]^{4-}$ oxidation potential. Solutions for measurements were prepared as follows: 20 (or 10) µL of 1 mmol L^{-1} stock solution of studied compound and 80 (or 90) µL of DMSO were pipetted into a vial and filled with phosphate buffer pH 7.2 to the final volume 1.0 mL. Solution was then transferred to a voltammetric cell. In the case of reducible substances **8a-c** oxygen was removed by 5min purging with nitrogen. CV scans were repeated at least 3 times for every single compound with the pre-treatment of GCE in-between scans. Potentials were evaluated at the point of maximum peak height for every single peak in CV. Parameters of fitted curves were evaluated by OriginPro 2016 software and they are reported at 0.95 confidence level.

2.3. In vitro antimycobacterial evaluation

The methodology of *in vitro* antimycobacterial activity screening of the investigated compounds **1-8c** against *Mycobacterium marinum* CAMP 5644, *M. kansasii* DSM 44162 and *M. smegmatis* ATCC 700084 was described in [5] and minimum inhibitory concentration (MIC) values are shown in Table 1.

Mycobacterium tuberculosis ATCC 25177/H37Ra was grown in Middlebrook broth (MB), supplemented with Oleic-Albumin-Dextrose-Catalase (OADC) supplement (Difco, Lawrence, KS, USA). At log phase growth, a culture sample (10 mL) was centrifuged at 15,000 rpm/20 min using a bench top centrifuge (MPW-65R, MPW Med Instruments, Warszawa, Poland). Following the removal of the supernatant, the pellet was washed in fresh Middlebrook 7H9GC broth and resuspended in fresh OADC-supplemented MB (10 mL). The turbidity was adjusted with MB to match McFarland standard No. 1 (3×10^8 CFU). A further 1:10 dilution of the culture was then performed in MB. The antimicrobial susceptibility of *M. tuberculosis* was investigated in a 96-well plate format. In these experiments, sterile deionized water (300 µL) was added to all outer-perimeter wells of the plates to minimize evaporation of the medium in the test wells during incubation. Each evaluated compound (100 µL) was incubated with *M. tuberculosis* (100 µL). Dilutions of each compound were prepared in duplicate. For all synthesized compounds, final concentrations ranged from 256 to 2 µg mL^{-1}. All compounds were dissolved in DMSO, and subsequent dilutions were made in supplemented MB. The plates were sealed with Parafilm and incubated at 37 °C for 14 days. Following the incubation, a 10% addition of alamarBlue (Difco) was mixed into each well, and readings at 570 nm and 600 nm were taken, initially for background subtraction and subsequently after 24 h reincubation. The background subtraction is necessary for strongly colored compounds, where the color may interfere with the interpretation of any color change. For noninterfering compounds, a blue color in the well was interpreted as the absence of growth, and a pink color was scored as growth. Isoniazid (Sigma) was used as the positive control, as it is a clinically used antitubercular drug. The results are shown in Table 1.

2.4. Study of inhibition of photosynthetic electron transport (PET) in spinach chloroplasts

The methodology of the evaluation of ring-substituted 1-hydroxynaphthalene-2-carboxanilides **1-8c** related to the inhibition of photosynthetic electron transport (PET) in spinach (*Spinacia oleracea* L.) chloroplasts was described in [5]. Inhibitory efficiency was expressed as IC_{50} values, see Table 1.

3. Results and discussion

3.1 Voltammetry in anodic area: Mechanism of oxidation

The phosphate buffer pH 7.2 – DMSO (9:1, v/v) medium was mostly used in this voltammetric study. It was the optimal medium for the voltammetric determination of the studied compound **8c** from our pilot study [26]. These conditions also provide similar pH that was used for *in vitro* screening of studied compounds, and it is also very close to physiological conditions. DMSO had to be used because of a limited solubility of compounds in aqueous media.

All the compounds gave one anodic oxidation response (Ia) ranging from ca. 200 to 400 mV vs. Ag/AgCl. Mechanism of the oxidation was closely studied with an unsubstituted compound **1** and conclusions from our previous study of the compound **8c** were also utilized [26]. The cyclic voltammogram in anodic area of the compound **1** is shown in Fig. 1. The compound **1** gave the peak Ia at 417 mV in the forward scan. In the reverse scan, products of the oxidation were reduced at the potential 181 mV at the peak Ic. In the second sweep a new peak IIa appeared at 208 mV and the height of the peak Ia was significantly decreased. Heights of all peaks were slowly decreasing during multiple consecutive scans probably due to the passivation of the electrode surface. A study by cyclic voltammetry with scan rates 10 – 1000 mV s^{-1} suggested that process Ia was diffusion controlled (until scan rate 200 mV s^{-1}) and the process IIa was controlled by adsorption. The current of the peak Ic did not correlate well with either scan rate or its square root, therefore mixed adsorption/diffusion control is presumed. The potential of the peak Ia was shifted to more positive potentials with the increasing scan rate as expected from an irreversible process. However, potentials of peaks Ic and IIa remained the same. The current ratio of *i*(Ia):*i*(Ic) was around 2:1 and it was independent on the scan rate.

All the compounds should exhibit the same pH dependency of the voltammetric response similar to the compound **8c** from our previous study [26]. The potential of the peak Ia depended on pH in neutral and slightly alkaline media with a slope close to −59 mV pH^{-1} ($1e^-/1H^+$ oxidation) suggesting a deprotonation step in the oxidation mechanism [26]. The oxidation potential was independent on pH in alkaline media, meaning that the compound (hydroxyl group) was already in the deprotonated form (given by pK_a of the compound). Cyclic voltammetry of the compound **1** carried out in an alkaline buffer pH 11 – DMSO (9:1, v/v) medium gave only two peaks during multiple scans. There was the peak Ia in the forward scan and the peak Ic in the reverse scan. However, peak IIa for adsorbed species in the second sweep was not observed.

From the literature concerning the oxidation of phenolic compounds [27-29] we can suggest, that the process Ia should be an irreversible process corresponding to the first step of the oxidation to a radical according to Scheme 2. Generated radicals in following reactions can either react with components of the solution or create polymer films that contribute to the passivation of the electrode surface. Peaks Ic, and IIa therefore correspond to adsorption processes involving adsorbed molecules created from previous reactions.

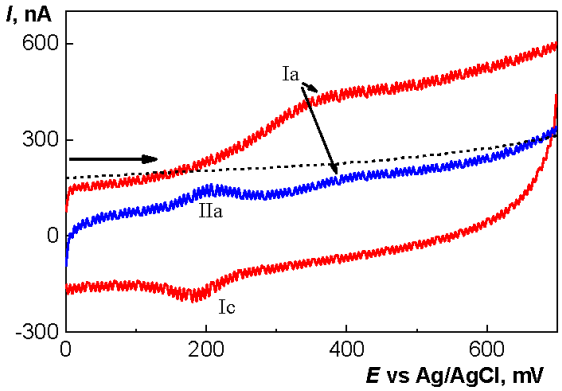

Fig. 1: Cyclic voltammogram (scan rate 50 mV s^{-1}) of compound **1** (c= 20 µmol L^{-1}) obtained on GCE in phosphate buffer pH 7.2 and DMSO (9:1, v/v) medium. The first cycle (red line) and forward scan of the second cycle (blue) are shown (reverse scan of the second cycle is the same as the first one). Forward scan of the supporting electrolyte is illustrated as a black dotted line. The arrow denotes the start and the direction of a scan from 0 V.

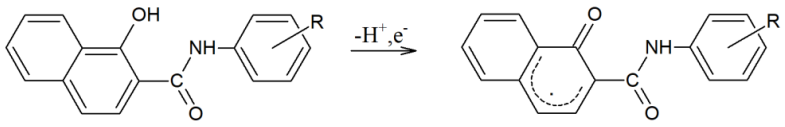

Scheme 2: Proposed first step of mechanism of the oxidation of compounds **1-8c** on GCE in the phosphate buffer pH 7.2 and DMSO (9:1, v/v) medium.

3.2 Voltammetry in anodic area: Relation of oxidation potential and Hammett σ values

As mentioned before, compounds **1-8c** were studied by the method of CV in the phosphate buffer pH 7.2 – DMSO medium (9:1, v/v). Experimentally obtained values of peaks Ia and Ic are shown in Table 1. Scan rate 50 mV s^{-1} was used because at that scan rate process Ia is still diffusion controlled which is a requirement for application of Hammett correlations.

All the studied compounds gave peaks corresponding to the signals obtained for the compound **1** described in the previous chapter, but respective potentials of observed peaks were different and characteristic for every substituent and its position. The proposed

mechanism of oxidation was the same for every compound and no irregularities were observed, concluding that substituents do not participate in the redox reaction (apart from compounds **8a-c** that contain a reducible nitro group at far more negative potentials; see chapter 3.4). The only difference in oxidation potentials of the hydroxyl moiety on the naphthalene ring was therefore caused by electron withdrawing or electron donating effects of various substituents on the benzene ring (or sum of inductive and mesomeric effects).

Monosubstituted derivatives are going to be discussed in three groups based on the position of the substituent (*ortho*, *meta*, *para*) for the purpose of finding a relation between the structure and the electrochemical potential. Hammett σ substituent values were adapted from [5] and they were correlated with experimentally obtained values of potentials for the peak Ia and the peak Ic from the reverse scan. As can be seen from plots for *ortho*- (Fig. 2A), *meta*- (Fig. 2B), and *para*- (Fig. 2C) substituted compounds, it is possible to establish a linear correlation between σ values and the potential of oxidation. The potential of the peak Ia of *ortho*- and *para*- derivatives gave linear dependency with similar slopes: −104±24 mV (r = −0.8866); −99±24 mV (r = −0.8789), respectively. However, unsubstituted compound **1** had to be excluded from both of correlations as an outlier. *Meta*- derivatives gave linear dependency with a higher slope value −163±35 mV (r = −0.8855), but with the unsubstituted compound **1** included in the correlation. All calculated slopes were significantly different from 0 (at 0.95 confidence level); therefore, there is a very good correlation in measured data between Hammett σ substituent constants and oxidation potential. Electron donating substituents -CH_3 and -OCH_3 caused a peak shift to more positive potentials, while on the other side electron withdrawing substituents -NO_2 and -CF_3 caused a peak shift towards 0 V, facilitating the oxidation. Halogen derivatives having -F, -Cl, and -Br as a weak electron withdrawing substituent had the oxidation potential in-between. Unsubstituted compound **1** gave the most positive potential. The value of a slope indicates how strongly a substituent affects the oxidation of a compound [33]. These findings suggest that electron withdrawing and donating effects of substituents on the benzene ring are significantly influencing electron density at the hydroxyl group on the naphthalene ring connected to the benzene ring with the –CONH– bridge. Additionally, a significant difference between slopes of *ortho*/*para* and *meta* derivatives was caused by well-known difference of inductive effect causing a change in electron density which is similar for *ortho*/*para* position contrary to *meta* position.

Similarly, dependencies of more positive cathodic peak Ic were evaluated (Fig. 2) but they gave lower slope values; in the case of *meta*-derivatives, a slope that was not even significantly different from 0. Therefore, for further discussion only potentials of the peak Ia are investigated.

Slight deviations from linear trend might be caused by varying adsorption or sterical effects of the respective compounds. In an ideal case, it should only be applied to diffusion processes [33]. In this case, adsorption processes also have to be considered based on a significant hydrophobicity of compounds. However, very good correlations were observed (r ~ 0.88), even though the studied substituents were on the secondary aromatic structure connected by –CONH– bridge.

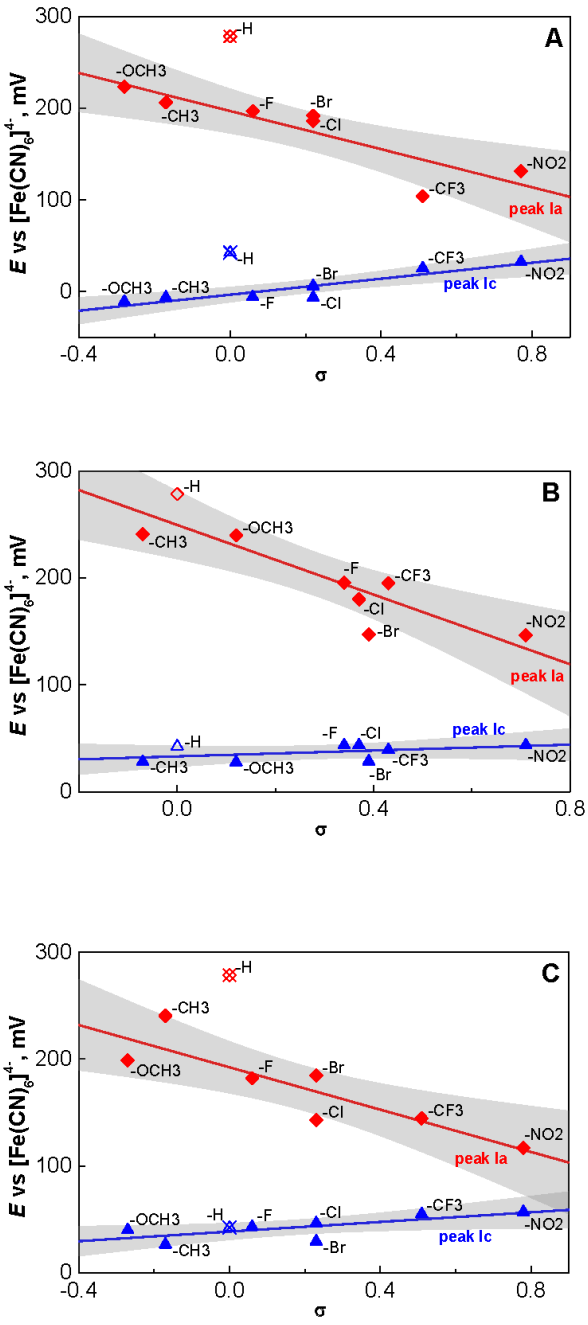

Fig. 2: Plot of potentials of anodic peak Ia (red) and cathodic reverse peak Ic (blue) *vs.* Hammett σ substituent constants of *ortho*- (A); *meta*- (B); and *para*- (C) substituted compounds **1-8c** obtained from Table 1. Linear straight lines correspond to linear fits; shaded

9

areas illustrate confidence intervals at 0.95 level. Crossed-out unsubstituted compound **1** in A and C was not included in a linear fit. Linear fit parameters are summarized in Table 2.

Table 1: Measured anodic potentials of signals Ia and Ic from CVs of ring-substituted 1-hydroxynaphthalene-2-carboxanilides **1-8c** and their calculated Hammett σ substituent constants, *in vitro* antimycobacterial activities (MICs) of compounds adapted from [5], new MICs against *M. tuberculosis* and IC_{50} values related to PET inhibition in spinach chloroplasts.

Compd	R-	σ[a]	E[b], mV		MIC, μmol L^{-1}				PET IC_{50}, μmol L^{-1}
			Ia	Ic	MM[c]	MK[d]	MS[e]	MT[f]	
1	H	0	279	43	60.7	15.2	243	60.8	31.3
2a	2-OCH_3	−0.28	224	−11	>873	>873	>873	>873	199.6
2b	3-OCH_3	0.12	240	28	54.5	>873	>873	54.5	23.5
2c	4-OCH_3	−0.27	199	40	>873	>873	>873	>873	79.5
3a	2-CH_3	−0.17	207	−7	28.8	115	231	231	62.8
3b	3-CH_3	−0.07	241	28	28.8	28.8	57.7	28.8	20.0
3c	4-CH_3	−0.17	241	27	115.0	57.7	923	462	28.7
4a	2-F	0.06	197	−6	56.8	>910	228	56.9	57.0
4b	3-F	0.34	196	44	28.4	28.4	910	28.4	15.6
4c	4-F	0.06	182	43	114.0	14.2	>910	114	20.3
5a	2-Cl	0.22	186	−7	107.0	860	860	430	29.4
5b	3-Cl	0.37	180	44	107.0	26.8	>860	26.9	7.9
5c	4-Cl	0.23	143	47	215.0	26.8	215	430	10.8
6a	2-Br	0.22	192	6	>748	>748	>748	>748	61.9
6b	3-Br	0.39	147	29	>748	>748	>748	93.6	8.2
6c	4-Br	0.23	185	30	46.7	23.3	46.7	>748	9.6
7a	2-CF_3	0.51	104	26	96.6	>773	>773	23.4	126.1
7b	3-CF_3	0.43	195	39	46.7	>748	>748	11.7	5.3
7c	4-CF_3	0.51	145	55	187.0	23.3	>748	23.4	36.5
8a	2-NO_2	0.77	132	33	>830	>830	>830	415	ND[g]
8b	3-NO_2	0.71	147	44	>830	>830	>830	>830	19.9
8c	4-NO_2	0.78	117	57	104.0	51.9	>830	>830	24.0

[a]- calculated using ACD/Percepta ver. 2012 (Advanced Chemistry Development, Inc., Toronto, ON, Canada, 2012); adapted from [5]
[b]- Potentials reported vs $[Fe^{II}(CN)_6]^{4-}$
[c]- MM = *M. marinum* CAMP 5644; adapted from [5]
[d]- MK = *M. kansasii* DSM 44162; adapted from [5]
[e]- MS = *M. smegmatis* ATCC 700084; adapted from [5]
[f]- MT = *M. tuberculosis* ATCC 25177/H37Ra
[g]- ND = not determined, see chapter 3.3

3.3 Relation between oxidation potential and biological activity

The evaluation of the *in vitro* antimycobacterial activity of compounds **1-8c** was performed against *Mycobacterium marinum* CAMP 5644, *M. kansasii* DSM 44162 and *M. smegmatis* ATCC 700084, see Table 1. The MIC values (minimum inhibitory concentration; lowest concentration at which no visible bacterial growth is observed) were taken from Gonec et al. [5]. In addition, all the compounds were evaluated against *M. tuberculosis* ATCC

25177/H37Ra. Avirulent strain *M. tuberculosis* ATCC 25177/H37Ra has a similar pathology as *M. tuberculosis* strains infecting humans [45], and simultaneously with *M. marinum*, both strains are commonly used model pathogens in basic laboratory screening for reduction of risks of laboratory workers [5]. *M. kansasii* DSM 44162 was used as a representative of non-tuberculous mycobacteria, causing the most frequent non-tuberculous mycobacterial lung infections [46]. All these strains belong to slow-growing species contrary to *M. smegmatis*, which is an ideal representative of a fast-growing non-pathogenic microorganism particularly useful in studying basic cellular processes of special relevance to pathogenic mycobacteria [5, 46].

Antimycobacterial activities of the compounds against individual tested strains were expressed as log(1/MIC) and were plotted against anodic oxidation potentials expressed as *E*(Ia), illustrated in Fig. 3–5 for the purpose of finding a relationship between the antimycobacterial activity and the potential. Note that only compounds with exact MIC values are illustrated in graphs. All the compounds were completely inactive against fast-growing *M. smegmatis* with the exception of compounds **6c** (R = 4-Br) and **3b** (R = 3-CH_3), that showed approx. 2.5-fold higher potency than isoniazid (commonly used drug for TB treatment); their *E*(Ia) values are 185 and 241 mV, respectively. Due to a small number of effective compounds, any dependence of the activity on the anodic potential was difficult to predict.

After elimination of all inactive compounds (MIC > 100 μmol L^{-1}) from following correlations (activities against *M. marinum*, *M. kansasii* and *M. tuberculosis*), only around 10 active compounds were left to investigate their relation to oxidation potentials. This amount proved to be too small to provide any definitive conclusions; anyway, it was still possible to outline some trends that could be useful in establishing a relation between activity and potential. This was illustrated on dependencies of activity against *M. marinum* and *M. kansasii* (after elimination of inactive compounds and unsubstituted **1**). Dependence of potential on activity against *M. marinum* (Fig. 3A) gave a quasi-parabolic trend (r = 0.7530, n = 9). This trend had a maximum around potentials 195-206 mV (compounds **3a** and **4b**). Dependency of the potential and the activity against *M. kansasii* (Fig. 3B) was also fitted with a quasi-parabolic trend (r = 0.7716, n = 9) with a maximum around potential 182 mV (compound **4c**).

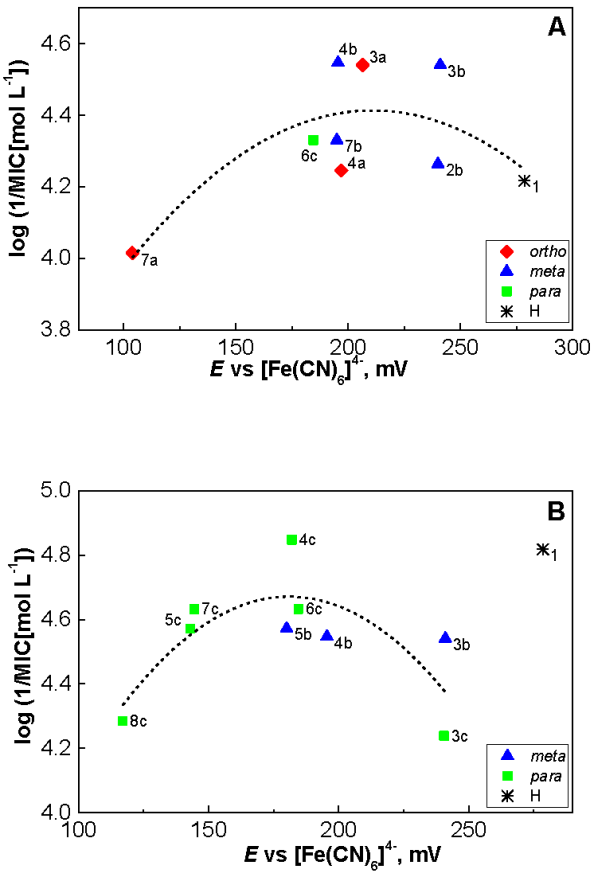

Fig. 3. Plot of log(1/MIC [mol L^{-1}]) of *in vitro* antimycobacterial activity against *M. marinum* (A) and *M. kansasii* (B) vs. potential of anodic peak *E*(Ia) of selected compounds **1-8c**; values obtained from Table 1. Dashed line represents quasi-parabolic trend. Polynomial fit parameters are given in Table 2.

1-Hydroxy-*N*-(3-trifluoromethylphenyl)naphthalene-2-carboxamide (**7b**) demonstrated the highest effectivity (MIC = 11.7 μmol L^{-1}) against *M. tuberculosis*. Additionally, other compounds, such as **7a** (R = 2-CF_3), **7c** (R = 4-CF_3), **5b** (R = 3-Cl), **3b** (R = 3-CH_3) and **4b** (R = 3-F) also showed high potency in the range from 23.4 to 28.8 μmol L^{-1}. Since MIC of isoniazid against *M. tuberculosis* is 36.6 μmol L^{-1}, it can be stated that the above-mentioned compounds expressed higher potency than the standard. Nevertheless, it is evident that the activity against *M. tuberculosis* is, in general, connected with CF_3 substitution of the anilide ring. On the other hand, *meta* position of substitution was the most advantageous similar to the case of *M. marinum,* but contrary to *M. kansasii*, where *para* position of substitution on the anilide ring is preferable [5]. A quasi-parabolic trend with a good correlation (r = 0.8620,

n = 6) was found (Fig. 4) only for a subset of *meta* derivatives with a maximum at the potential 195 mV (compound **7b**). The only active *ortho* and *para* compounds in the order **7a**, **7c**, **4a**, **1** had a decreasing activity with higher oxidation potential; however, no reliable conclusions can be drawn from this trend.

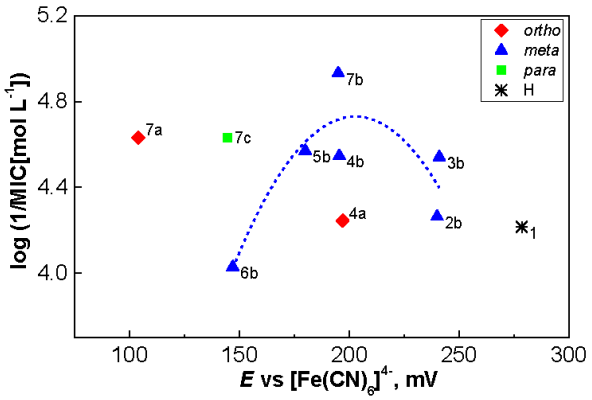

Fig. 4. Plot of log(1/MIC [mol L^{-1}]) of *in vitro* antimycobacterial activity against *M. tuberculosis* vs. potential of anodic peak *E*(Ia) of selected compounds **1-8c**; values obtained from Table 1. Dashed line represents quasi-parabolic trend only for *meta* subset. Polynomial fit parameters are given in Table 2.

As mentioned above, these compounds were additionally tested for their ability to inhibit photosynthetic electron transport (PET) in spinach (*Spinacia oleracea* L.) chloroplasts. PET inhibiting activity expressed as IC_{50} value (compound concentration causing 50% inhibition of PET) was taken from Gonec et al. [5] (Table 1). Compound **7b** was the most effective (IC_{50} = 5.3 μmol L^{-1}), slightly worse than the selective herbicide 3-(3,4-dichlorophenyl)-1,1-dimethylurea, DCMU (Diurone®) with IC_{50} = 1.9 μmol L^{-1}. It was not possible to determine IC_{50} value for the compound **8a** (R = 2-NO_2) due to its interactions during the measurement. Compound **2a** (R = 2-OCH_3) expressed the lowest PET-inhibiting activity (IC_{50} = 199.6 μmol L^{-1}), although, in general, it can be stated that *ortho*-substituted subset expressed the lowest PET inhibition in the comparison with *meta*- and *para*-substituted subsets. Within these two subsets, compounds **2c** (R = 4-OCH_3) and **7c** (R = 4-CF_3) showed the lowest potency (IC_{50} = 79.5 and 36.5 μmol L^{-1}, respectively), therefore, similarly as in Gonec et al. [5], these compounds were excluded from the search of relationship between PET-inhibiting activity and the oxidation potential. The dependences of PET inhibition expressed as log(1/IC_{50}) on the anodic potential *E*(Ia) of the compounds are shown in Fig. 5. Even though *ortho* subset exhibits lowest activity, it gives very clear steep linear dependency on the potential (r = 0.9373, n = 5). In addition, both *meta* and *para* substituted compounds gave quasi-parabolic trend (r = 0.6925, n = 12) with maximum activity between potentials 180 to 195 mV. Furthermore, an above-mentioned presumption about a correlation between PET

inhibition and the antimycobacterial activity [5-11, 15, 23-25] can be outlined based on these results. This can be seen for effective compounds **7b** (R = 3-CF_3), **5b** (R = 3-Cl), **4b** (R = 3-F) and **3b** (R = 3-CH_3); while, more importantly, compounds **3b** and **4b** were active in all performed tests.

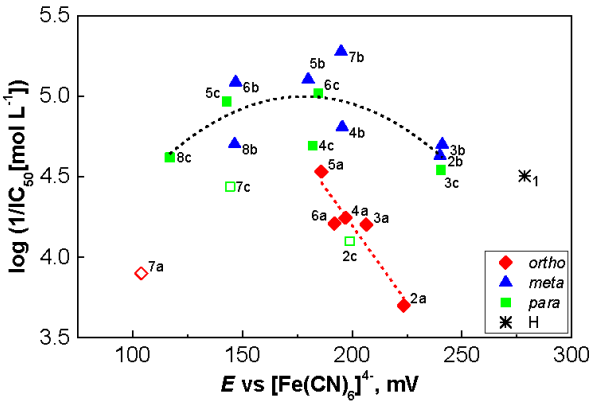

Fig. 5. Plot of log(1/IC_{50} [mol L^{-1}]) of PET inhibition in spinach chloroplasts vs. potential of anodic peak *E*(Ia) of selected compounds **1-8c**; values obtained from Table 1. Eliminated compounds are marked by an empty symbol. Dashed lines represent quasi-parabolic trend only for *meta* and *para* subset (black) and linear trend for *ortho* subset only (red). Fit parameters are given in Table 2.

Table 2: Parameters of calculated linear dependencies of potentials *E*(Ia) and *E*(Ic) on Hammett σ substituent constants and polynomial dependencies of antimycobacterial activity MIC values for *M. marinum* (*M.m*), *M. kansasii* (*M.k.*) and *M. tuberculosis* (*M.t.*) and PET IC_{50} values on the potential *E*(Ia).

Hammett correlations: x = a × σ + b					
From Fig.	x, mV	a, mV	b, mV	r	
2A	*E*(Ia, *ortho*)	−104 (±24)	197 (±10)	−0.8866	
2A	*E*(Ic, *ortho*)	43.7 (±8.3)	−3.4 (±3.2)	0.9204	
2B	*E*(Ia, *meta*)	−163 (±35)	250 (±13)	−0.8855	
2B	*E*(Ic, *meta*)	14 (±11)	33.1 (±4.0)	0.4606	
2C	*E*(Ia, *para*)	−99 (±24)	192.3 (±9.4)	−0.8789	
2C	*E*(Ic, *para*)	22.5 (±8.7)	38.6 (±3.2)	0.7260	
Activity-structure correlations: x = a ×10^{-5} × E^2(Ia) + b ×10^{-2} × *E*(Ia) + c					
From Fig.	x	a, mV^{-2}	b, mV^{-1}	c	r
3A	log(1/MIC(*M.m.*))	−3.6 (±1.5)	1.52 (±0.58)	2.81 (±0.55)	0.7530
3B	log(1/MIC(*M.k.*))	−8.2 (±2.8)	3.0 (±1.0)	1.97 (±0.91)	0.7716
4	log(1/MIC(*M.t.*), *meta*)	−23 (±8.0)	9.2 (±3.2)	−4.6 (±3.1)	0.8621
5	log(1/IC_{50}, *meta*+*para*)	−9.5 (±3.6)	3.4 (±1.3)	2.0 (±1.2)	0.6925
5	log(1/IC_{50}, *ortho*)	-	−1.92 (±0.41)	8.03 (±0.83)	−0.9373

*3.4 Voltammetry in cathodic area: Relation of potential on structure and biological activity of compounds **8a-c***

Only 3 of studied compounds **8a-c** contain a nitro moiety (reducible at GCE), therefore they will be discussed only briefly. Cyclic voltammogram of the compound **8b** is shown in Fig. 6. Compounds **8a-c** gave one cathodic response (IIIc) corresponding to the well-known 4-electron reduction to the hydroxylamine that is reversibly oxidized to the nitroso compound in a reverse scan (pair of peaks IVa/IVc) [27, 31]. This mechanism of reduction was investigated in detail in our previous publication with the compound **8c** [26].

Regrettably, nitro derivatives **8a-c** did not show any antimicrobial activity (Table 3), despite many different compounds with a nitro moiety exhibiting high antimycobacterial and/or antibacterial effects such as 5-nitroimidazoles (e.g., metronidazole, ornidazol, tinidazol) and 5-nitrofurans (e.g., nitrofurantoin, nifurantel, nifuroxazid), where a nitro moiety is a crucial structural factor for the high activity. Effectivity of a new class of antimycobacterial drugs derived from nitroimidazole, such as delamanid and pretomanid, is also based on the presence of a nitro moiety [4]. From this point of view, the biological activity of these derivatives was disappointing. Therefore, the only valid conclusion into a relationship between the structure and the reduction potential IIIc of compounds **8a-c** is as follows. The reduction is facilitated in a series *para*→*meta*→*ortho*, with *ortho*-substituted compound having the potential closest to 0 V, as summarized in Table 3.

It should be noted that in the previous paper, where antiproliferative activity of these compounds was investigated [14], the potential of reversible peaks IVa/IVc correlates with the cytotoxicity against normal human fibroblast cell line (NHDF), where the compound **8a** (R = 2-NO_2) showed IC_{50} = 22.71±2.71 μmol L^{-1}, the compound **8b** (R = 3-NO_2) IC_{50} > 25 μmol L^{-1} and the compound **8c** (R = 4-NO_2) IC_{50} = 12.30±1.49 μmol L^{-1} [14]. It can be summarized that cytotoxic potential against human cells within these nitro derivatives increases with decreasing potential *E*(IVa/IVc) as follows: −242 mV (R = 3-NO_2, **8b**) < −268 mV (R = 2-NO_2, **8a**) < −292 mV (R = 4-NO_2, **8c**).

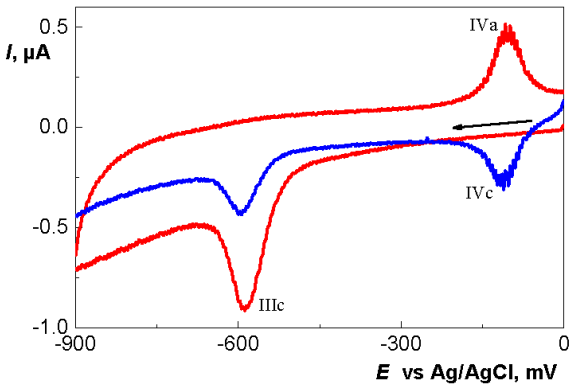

Fig. 6: Cyclic voltammogram (scan rate 50 mV s^{-1}) of compound **8b** (c = 10 µmol L^{-1}) obtained on GCE in phosphate buffer pH 7.2 and DMSO (9:1, v/v) medium. The first cycle (red line) and forward scan of the second cycle (blue) are shown (reverse scan of the second cycle is the same as the first one). The arrow denotes the start and the direction of a scan from 0 V.

Table 3: Measured cathodic potentials of signals IIIc and reversible pair IVa/IVc from CV of NO_2-substituted 1-hydroxynaphthalene-2-carboxanilides **8a-c** and their IC_{50} values related to PET inhibition in spinach chloroplasts; *in vitro* antimycobacterial activity (MIC) of compounds adapted from [5].

Compd	R-	E[a], mV		MIC, µmol L^{-1}				PET IC_{50}, µmol L^{-1}
		IIIc	IVa/IVc	MM[b]	MK[c]	MS[d]	MT[e]	
8a	2-NO_2	−690	−268	>830	>830	>830	415	ND[f]
8b	3-NO_2	−721	−242	>830	>830	>830	>830	19.9
8c	4-NO_2	−755	−292	104	51.9	>830	>830	24.0

[a]- Potentials reported vs $[Fe^{II}(CN)_6]^{4-}$
[b]- MM = *M. marinum* CAMP 5644; adapted from [5]
[c]- MK = *M. kansasii* DSM 44162; adapted from [5]
[d]- MS = *M. smegmatis* ATCC 700084; adapted from [5]
[e]- MT = *M. tuberculosis* ATCC 25177/H37Ra
[f]- ND = not determined, see chapter 3.3

4. Conclusion

Twenty-two novel antimycobacterial agents were investigated by cyclic voltammetry. The hydroxyl group on the naphthalene moiety gave one irreversible oxidation signal and its potential ranged from 104 mV (**7a**, R = 2-CF_3) to 279 mV (**1**, R = H) (vs. $[Fe^{II}(CN)_6]^{4-}$). Relationships between the structure (Hammett σ substituent constant) and the oxidation potential was established with satisfactory correlation coefficients (r ~ 0.88), that was associated with electron donating or withdrawing capabilities of given substituents and their position. In general, electron donating substituents caused a shift to more positive potentials and vice versa. Correlations between the oxidation potential and *in vitro* antimycobacterial activity of selected mycobacterial pathogens mostly gave quasi-parabolic dependencies with good correlation coefficients (approx. r ~ 0.7-0.8) and with maxima usually in the range 180-195 mV. However, two most active compounds **3b** (R = 3-CH_3) and **4b** (R = 3-F) gave potential 196 mV and 241 mV, respectively, so in general, biological activity should be positively affected by higher oxidation potential.

Based on these results we can prove that the ease of oxidation of phenolic group can be used as one of many parameters that can help design of novel antibiotic agents. In the end, it is essential to remind that also a lot of other factors and physicochemical parameters, i.e. lipophilicity (as discussed in Gonec et al. [5]) have an undeniable effect on the drug effectivity.

Acknowledgments

J.G., K.T., J.B., and J.F. acknowledge the support of the Czech Science Foundation (17-03868S). J.G. thanks for the support of Specific University Research (SVV 260440). H.M., T.G., and J.J. acknowledge the support of the Ministry of Education of the Czech Republic (LO1305) and the Slovak Research and Development Agency (APVV-17-0373 and APVV-17-0318). M.B., Z.S. and M.F. acknowledge institutional support from the Czech Academy of Sciences (No. 68081707).

References

[1] World Health Organisation, Global tuberculosis report 2018, WHO Press, Geneva, 2018.
[2] A. Koul, E. Arnoult, N. Lounis, J. Guillemont, K. Andries, The challenge of new drug discovery for tuberculosis, Nature 469 (2011) 483-490. http://doi.org/10.1038/nature09657
[3] D. Wagner, L.S. Young, Nontuberculous Mycobacterial Infections: A Clinical Review, Infection 32 (2004) 257-270. http://doi.org/10.1007/s15010-004-4001-4
[4] J. Jampilek, Design and Discovery of New Antibacterial Agents: Advances Perspectives, Challenges, Curr. Med. Chem. 25 (2018) 4972-5006. http://doi.org/10.2174/0929867324666170918122633
[5] T. Gonec, J. Kos, I. Zadrazilova, M. Pesko, S. Keltosova, J. Tengler, P. Bobal, P. Kollar, A. Cizek, K. Kralova, J. Jampilek, Antimycobacterial and herbicidal activity of ring-substituted 1-hydroxynaphthalene-2-carboxanilides, Bioorg. Med. Chem. 21 (2013) 6531-6541. http://doi.org/10.1016/j.bmc.2013.08.030
[6] J. Kos, I. Zadrazilova, M. Pesko, S. Keltosova, J. Tengler, T. Gonec, P. Bobal, T. Kauerova, M. Oravec, P. Kollar, A. Cizek, K. Kralova, J. Jampilek, Antibacterial and Herbicidal Activity of Ring-Substituted 3-Hydroxynaphthalene-2-carboxanilides, Molecules 18 (2013) 7977-7997. http://doi.org/10.3390/molecules18077977
[7] T. Gonec, J. Kos, I. Zadrazilova, M. Pesko, R. Govender, S. Keltosova, B. Chambel, D. Pereira, P. Kollar, A. Imramovsky, J. O'Mahony, A. Coffey, A. Cizek, K. Kralova, J. Jampilek, Antibacterial and Herbicidal Activity of Ring-Substituted 2-Hydroxynaphthalene-1-carboxanilides, Molecules 18 (2013) 9397-9419. http://doi.org/10.3390/molecules18089397
[8] T. Gonec, I. Zadrazilova, E. Nevin, T. Kauerova, M. Pesko, J. Kos, M. Oravec, P. Kollar, A. Coffey, J. Mahony, A. Cizek, K. Kralova, J. Jampilek, Synthesis and Biological Evaluation of N-Alkoxyphenyl-3-hydroxynaphthalene-2-carboxanilides, Molecules 20 (2015) 9767-9787. http://doi.org/10.3390/molecules20069767
[9] J. Kos, E. Nevin, M. Soral, I. Kushkevych, T. Gonec, P. Bobal, P. Kollar, A. Coffey, J. O'Mahony, T. Liptaj, K. Kralova, J. Jampilek, Synthesis and antimycobacterial properties of ring-substituted 6-hydroxynaphthalene-2-carboxanilides, Bioorg. Med. Chem. 23 (2015) 2035-2043. http://doi.org/10.1016/j.bmc.2015.03.018
[10] T. Gonec, S. Pospisilova, T. Kauerova, J. Kos, J. Dohanosova, M. Oravec, P. Kollar, A. Coffey, T. Liptaj, A. Cizek, J. Jampilek, N-Alkoxyphenylhydroxynaphthalenecarboxamides and Their Antimycobacterial Activity, Molecules 21 (2016) 1068. http://doi.org/10.3390/molecules21081068
[11] T. Gonec, S. Pospisilova, L. Holanova, J. Stranik, A. Cernikova, V. Pudelkova, J. Kos, M. Oravec, P. Kollar, A. Cizek, J. Jampilek, Synthesis and Antimicrobial Evaluation of 1- (2-

Substituted phenyl)carbamoyl naphthalen-2-yl Carbamates, Molecules 21 (2016) 1189. http://doi.org/10.3390/molecules21091189
[12] J. Kos, I. Kapustikova, C. Clements, A.I. Gray, J. Jampilek, 3-Hydroxynaphthalene-2-carboxanilides and their antitrypanosomal activity, Monatsh. Chem. 149 (2018) 887-892. http://doi.org/10.1007/s00706-017-2099-1
[13] T. Kauerova, J. Kos, T. Gonec, J. Jampilek, P. Kollar, Antiproliferative and Pro-Apoptotic Effect of Novel Nitro-Substituted Hydroxynaphthanilides on Human Cancer Cell Lines, Int. J. Mol. Sci. 17 (2016) 1219. http://doi.org/10.3390/ijms17081219
[14] E. Spaczynska, A. Mrozek-Wilczkiewicz, K. Malarz, J. Kos, T. Gonec, M. Oravec, R. Gawecki, A. Bak, J. Dohanosova, I. Kapustikova, T. Liptaj, J. Jampilek, R. Musiol, Design and synthesis of anticancer 1-hydroxynaphthalene-2-carboxanilides with a p53 independent mechanism of action, Sci. Rep. 9 (2019) 6387. http://doi.org/10.1038/s41598-019-42595-y
[15] A. Imramovsky, M. Pesko, J.M. Ferriz, K. Kralova, J. Vinsova, J. Jampilek, Photosynthesis-Inhibiting efficiency of 4-chloro-2-(chlorophenylcarbamoyl)phenyl alkylcarbamates, Bioorg. Med. Chem. Lett. 21 (2011) 4564-4567. http://doi.org/10.1016/j.bmcl.2011.05.118
[16] I. Zadrazilova, S. Pospisilova, K. Pauk, A. Imramovsky, J. Vinsova, A. Cizek, J. Jampilek, In Vitro Bactericidal Activity of 4- and 5-Chloro-2-hydroxy-N-[1-oxo-1-(phenylamino)alkan-2-yl]benzamides against MRSA, Biomed. Res. Int. 2015 (2015) 349534. http://doi.org/10.1155/2015/349534
[17] K. Pauk, I. Zadrazilova, A. Imramovsky, J. Vinsova, M. Pokorna, M. Masarikova, A. Cizek, J. Jampilek, New derivatives of salicylamides: Preparation and antimicrobial activity against various bacterial species, Bioorg. Med. Chem. 21 (2013) 6574-6581. http://doi.org/10.1016/j.bmc.2013.08.029
[18] I. Zadrazilova, S. Pospisilova, M. Masarikova, A. Imramovsky, J.M. Ferriz, J. Vinsova, A. Cizek, J. Jampilek, Salicylanilide carbamates: Promising antibacterial agents with high in vitro activity against methicillin-resistant Staphylococcus aureus (MRSA), Eur. J. Pharm. Sci. 77 (2015) 197-207. http://doi.org/10.1016/j.ejps.2015.06.009
[19] N.R. Baker, M.P. Percival, Herbicides, Topics in Photosynthesis, Vol. 10, Elsevier Science Publishers, Amsterdam, 1991.
[20] A. Koul, L. Vranckx, N. Dhar, H.W.H. Göhlmann, E. Özdemir, J.-M. Neefs, M. Schulz, P. Lu, E. Mørtz, J.D. McKinney, K. Andries, D. Bald, Delayed bactericidal response of Mycobacterium tuberculosis to bedaquiline involves remodelling of bacterial metabolism, Nat. Commun. 5 (2014) 3369. http://doi.org/10.1038/ncomms4369
[21] R.V. Bueno, R.C. Braga, N.D. Segretti, E.I. Ferreira, G.H.G. Trossini, C.H. Andrade, New Tuberculostatic Agents Targeting Nucleic Acid Biosynthesis: Drug Design using QSAR Approaches, Curr. Pharm. Design 20 (2014) 4474-4485. http://doi.org/10.2174/13816128196661311181702 38
[22] T. Gonec, J. Kos, E. Nevin, R. Govender, M. Pesko, J. Tengler, I. Kushkevych, V. Stastna, M. Oravec, P. Kollar, J. O'Mahony, K. Kralova, A. Coffey, J. Jampilek, Preparation and Biological Properties of Ring-Substituted Naphthalene-1-Carboxanilides, Molecules 19 (2014) 10386-10409. http://doi.org/10.3390/molecules190710386
[23] T. Gonec, K. Kralova, M. Pesko, J. Jampilek, Antimycobacterial N-alkoxyphenylhydroxynaphthalenecarboxamides affecting photosystem II, Bioorg. Med. Chem. Lett. 27 (2017) 1881-1885. http://doi.org/10.1016/j.bmcl.2017.03.050
[24] J. Jampilek, K. Kralova, M. Pesko, J. Kos, Ring-substituted 8-hydroxyquinoline-2-carboxanilides as photosystem II inhibitors, Bioorg. Med. Chem. Lett. 26 (2016) 3862-3865. http://doi.org/10.1016/j.bmcl.2016.07.021

[25] W. Oettmeier, Herbicides, Inhibitors of Photosynthesis at Photosystem II, in: J.R. Plimmer, N.N. Ragsdale, D. Gammon (Eds.), Encyclopedia of Agrochemicals, John Wiley & Sons, Hoboken, NJ, 2003.
[26] J. Gajdár, T. Goněc, J. Jampílek, M. Brázdová, Z. Bábková, M. Fojta, J. Barek, J. Fischer, Voltammetry of a Novel Antimycobacterial Agent 1-Hydroxy-N-(4-nitrophenyl)naphthalene-2-carboxamide in a Single Drop of a Solution, Electroanalysis 30 (2018) 38-47. http://doi.org/10.1002/elan.201700547
[27] J. Grimshaw, Electrochemical Reactions and Mechanisms in Organic Chemistry, Elsevier Science, Amsterdam, 2000.
[28] R. Francke, T. Quell, A. Wiebe, S.R. Waldvogel, Oxygen-Containing Compounds: Alcohols, Ethers, and Phenols, in: O. Hammerich, B. Speiser (Eds.), Organic Electrochemistry, CRC Press, Boca Raton, FL, 2016, p. 981-1033.
[29] J. Stradins, B. Hasanli, Anodic voltammetry of phenol and benzenethiol derivatives, J. Electroanal. Chem. 353 (1993) 57-69. http://doi.org/10.1016/0022-0728(93)80286-Q
[30] I. Rubinstein, Voltammetric Study of Nitrobenzene and Related Compounds on Solid Electrodes in Aqueous Solution, J. Electroanal. Chem. 183 (1985) 379-386. http://doi.org/10.1016/0368-1874(85)85503-9
[31] P. Zuman, Z. Fijalek, D. Dumanovic, D. Suznjevic, Polarographic and Electrochemical Studies of Some Aromatic and Heterocyclic Nitro Compounds, 1. General Mechanistic Aspects, Electroanalysis 4 (1992) 783-794. http://doi.org/10.1002/elan.1140040808
[32] O. Hammerich, Reduction of Nitro Compounds and Related Substrates, in: O. Hammerich, B. Speiser (Eds.), Organic Electrochemistry, CRC Press, Boca Raton, FL, 2016, p. 1150-1190.
[33] P. Zuman, Substituent Effects in Organic Polarography, Plenum Press, New York, 1967.
[34] J.E. Kuder, H.W. Gibson, D. Wychick, Electrochemical characterization of salicylaldehyde anils, J. Org. Chem. 40 (1975) 875-879. http://doi.org/10.1021/jo00895a013
[35] T. Mikysek, H. Kvapilová, F. Josefík, J. Ludvík, Electrochemical and Theoretical Study of a New Series of Bicyclic Oxazaborines, Anal. Lett. 49 (2016) 178-187. http://doi.org/10.1080/00032719.2015.1017761
[36] E. Moreno, S. Perez-Silanes, S. Gouravaram, A. Macharam, S. Ancizu, E. Torres, I. Aldana, A. Monge, P.W. Crawford, 1,4-Di-N-oxide quinoxaline-2-carboxamide: Cyclic voltammetry and relationship between electrochemical behavior, structure and anti-tuberculosis activity, Electrochim. Acta 56 (2011) 3270-3275. http://doi.org/10.1016/j.electacta.2011.01.030
[37] F.S.d. Paula, É.M. Sales, M. Vallaro, R. Fruttero, M.O.F. Goulart, The relationship between redox potentials and substituent constants in biologically active arylazoxy compounds, J. Electroanal. Chem. 579 (2005) 33-41. http://doi.org/10.1016/j.jelechem.2005.01.023
[38] K.R. Kunz, B.S. Iyengar, R.T. Dorr, D.S. Alberts, W.A. Remers, Structure activity relationship for mitomycin C and mitomycin A analogs, J. Med. Chem. 34 (1991) 2281-2286. http://doi.org/10.1021/jm00111a051
[39] P.W. Crawford, E. Carlos, J.C. Ellegood, C.C. Cheng, Q. Dong, D.F. Liu, Y.L. Luo, The electrochemistry of antineoplastic furanquinones: Electrochemical properties of benzo[b]naphtho[2,3-d]furan-6,11-dione derivatives, Electrochim. Acta 41 (1996) 2399-2403. http://doi.org/10.1016/0013-4686(96)00020-5
[40] P. Kovacic, J.R. Ames, M.D. Ryan, Reduction potentials of antimycobacterial agents: Relationship to activity, Bioelectroch. Bioener. 21 (1989) 269-278. http://doi.org/10.1016/0302-4598(89)85006-8
[41] J. Jampilek, Recent Advances in Design of Potential Quinoxaline Anti-Infectives, Curr. Med. Chem. 21 (2014) 4347-4373. http://doi.org/10.2174/09298673216661410111948 25

[42] G. Dryhurst, Electrochemistry and Biological Processes, in: G. Dryhurst (Ed.), Electrochemistry of Biological Molecules, Academic Press, New York, NY, 1977, p. 1-5.
[43] R.J. Driebergen, E.E. Moret, L.H.M. Janssen, J.S. Blauw, J.J.M. Holthuis, S.J. Postma Kelder, W. Verboom, D.N. Reinhoudt, W.E. van der Linden, Electrochemistry of potentially bioreductive alkylating quinones: Part 3. Quantitative structure-electrochemistry relationships of aziridinylquinones, Anal. Chim. Acta 257 (1992) 257-273. http://doi.org/10.1016/0003-2670(92)85179-A
[44] F.C.d. Abreu, P.A.d.L. Ferraz, M.O.F. Goulart, Some Applications of Electrochemistry in Biomedical Chemistry. Emphasis on the Correlation of Electrochemical and Bioactive Properties, J. Brazil. Chem. Soc. 13 (2002) 19-35. http://doi.org/10.1590/S0103-50532002000100004
[45] M.T. Heinrichs, R.J. May, F. Heider, T. Reimers, S.K.B. Sy, C.A. Peloquin, H. Derendorf, Mycobacterium tuberculosis Strains H37ra and H37rv have Equivalent Minimum Inhibitory Concentrations to Most Antituberculosis Drugs, Int. J. Mycobact. 7 (2018) 156-161. http://doi.org/10.4103/ijmy.ijmy_33_18
[46] J.R. Honda, R. Virdi, E.D. Chan, Global Environmental Nontuberculous Mycobacteria and Their Contemporaneous Man-Made and Natural Niches, Front. Microbiol. 9 (2018) 2029. http://doi.org/10.3389/fmicb.2018.02029

10. APPENDIX V – CONFIRMATION OF PARTICIPATION

I. **Gajdár J.**, Barek J., Fojta M., Fischer J.: Micro volume voltammetric determination of 4-nitrophenol in dimethyl sulfoxide at a glassy carbon electrode. Monatshefte für Chemie - Chemical Monthly *148*, 1639-1644 (2017).
Impact factor (2018): **1.501**; Percentage of participation of Mgr. Július Gajdár ~**85 %**

II. **Gajdár J.**, Goněc T., Jampílek J., Brázdová M., Bábková Z., Fojta M., Barek J., Fischer J.: Voltammetry of a novel antimycobacterial agent 1-hydroxy-*N*-(4-nitrophenyl)naphthalene-2-carboxamide in a single drop of a solution. Electroanalysis *30*, 38-47 (2018).
Impact factor (2018): **2.691**; Percentage of participation of Mgr. Július Gajdár ~**65 %**

III. **Gajdár J.**, Barek J., Fischer J.: Electrochemical microcell based on silver solid amalgam electrode for voltammetric determination of pesticide difenzoquat. Sensors and Actuators B: Chemical *299*, 126931 (2019).
Impact factor (2018): **6.393**; Percentage of participation of Mgr. Július Gajdár ~**85 %**

IV. **Gajdár J.**, Tsami K., Michnová H., Goněc T., Brázdová M., Soldánová Z., Fojta M., Jampílek J., Barek J., Fischer J.: Electrochemistry of ring-substituted 1-hydroxynaphthalene-2-carboxanilides: Relation to structure and biological activity. Electrochimica Acta, *submitted* (2019).
Impact factor (2018): **5.383**; Percentage of participation of Mgr. Július Gajdár ~**35 %**

I declare that the percentage of participation of Mgr. Július Gajdár at the above given papers corresponds to above given numbers.

Prague, 9. 10. 2019 prof. RNDr. Jiří Barek, CSc.

11. APPENDIX VI – LIST OF PUBLICATIONS, ORAL AND POSTER PRESENTATIONS, AND INTERNSHIPS

A) List of journal articles:

1. **Gajdár J.**, Barek J., Fischer J.: Antimony film electrodes for voltammetric determination of pesticide trifluralin. Journal of Electroanalytical Chemistry *778*, 1-6 (2016).

2. **Gajdar J.**, Horakova E., Barek J., Fischer J., Vyskocil V.: Recent applications of mercury electrodes for monitoring of pesticides: A critical review. Electroanalysis *28*, 2659-2671 (2016).

3. **Gajdár J.**, Barek J., Fojta M., Fischer J.: Micro volume voltammetric determination of 4-nitrophenol in dimethyl sulfoxide at a glassy carbon electrode. Monatshefte für Chemie - Chemical Monthly *148*, 1639-1644 (2017).

4. **Gajdár J.**, Goněc T., Jampílek J., Brázdová M., Bábková Z., Fojta M., Barek J., Fischer J.: Voltammetry of a novel antimycobacterial agent 1-hydroxy-*N*-(4-nitrophenyl)naphthalene-2-carboxamide in a single drop of a solution. Electroanalysis *30*, 38-47 (2018).

5. **Gajdár J.**, Barek J., Fischer J.: Electrochemical microcell based on silver solid amalgam electrode for voltammetric determination of pesticide difenzoquat. Sensors and Actuators B: Chemical *299*, 126931 (2019).

6. **Gajdár J.**, Tsami K., Michnová H., Goněc T., Brázdová M., Bábková Z., Fojta M., Jampílek J., Barek J., Fischer J.: Electrochemistry of ring-substituted 1-hydroxynaphthalene-2-carboxanilides: Relation to structure and biological activity. Electrochimica Acta *submitted* (2019).

B) List of oral presentations:

1. **Gajdár J.**, Fischer J.: Využitie antimónových filmových elektród pre stanovenie pesticídu trifluralinu. *O cenu Karla Štulíka - Soutěž o nejlepší studentskou vědeckou práci v oboru analytická chemie,* Ostrava, Czech Republic (4.-5. February 2015).

2. **Gajdár J.**, Goněc T., Jampílek J., Brázdová M., Bábková Z., Fojta M., Barek J., Fischer J.: Voltammetry of 1-hydroxy-*N*-(4-nitrophenyl)naphthalene-2-carboxamide at a glassy carbon electrode. *36th International Conference on Modern Electrochemical Methods (MEM),* Jetřichovice, Czech Republic (23.-27. May 2016).
3. **Gajdár J.**, Goněc T., Jampílek J., Brázdová M., Bábková Z., Fojta M., Barek J., Fischer J.: Voltammetric determination of 1-hydroxy-*N*-(4-nitrophenyl)naphthalene-2-carboxamide by voltammetry at a glassy carbon electrode in microvolumes of dimethyl sulfoxide. *12th International Students Conference on Modern Analytical Chemistry,* Prague, Czech Republic (22.-23. September 2016).
4. **Gajdár J.**, Goněc T., Jampílek J., Brázdová M., Bábková Z., Fojta M., Barek J., Fischer J.: Determination of a novel antimycobacterial agent in a single drop of a solution by voltammetry at a glassy carbon electrode. *37th International Conference on Modern Electrochemical Methods (MEM),* Jetřichovice, Czech Republic (15.-19. May 2017).
5. **Gajdár J.**, Goněc T., Jampílek J., Brázdová M., Bábková Z., Fojta M., Barek J., Fischer J.: Voltammetric techniques for analysis in a single drop of a solution. *13th International Students Conference on Modern Analytical Chemistry,* Prague, Czech Republic (21.-22. September 2017).
6. **Gajdár J.**, Goněc T., Jampílek J., Brázdová M., Bábková Z., Fojta M., Barek J., Fischer J.: Voltammetric determination of electrochemically active compounds in micro volumes. *1st Cross-border Seminar on Electroanalytical Chemistry (CBSEC),* Furth im Wald, Germany (4.-6. April 2018).
7. **Gajdár J.**, Sarkar S, Mandler D., Fischer J., Barek J.: Voltammetry of electroactive species at the interface in Langmuir-Blodgett trough. *38th International Conference on Modern Electrochemical Methods (MEM),* Jetřichovice, Czech Republic (21.-25. May 2018).
8. **Gajdár J.**, Barek J., Fischer J.: Determination of difenzoquat at a mercury meniscus modified silver solid amalgam electrode by differential pulse voltammetry. *14th International Students Conference on Modern Analytical Chemistry,* Prague, Czech Republic (20.-21. September 2018).
9. **Gajdár J.**, Tsami K., Goněc T., Jampílek J., Brázdová M., Bábková Z., Fojta M., Barek J., Fischer J.: Cyclic voltammetry of biologically active hydroxynaphthalenecarboxanilides and its relationship to substituent constants. *2nd Cross-border Seminar on Electroanalytical Chemistry (CBSEC),* České Budějovice, Czech Republic (10.-12. April 2019).

10. **Gajdár J.**, Goněc T., Jampílek J., Brázdová M., Bábková Z., Fojta M., Barek J., Fischer J.: Cathodic voltammetric determination of a nitro substituted 1-Hydroxynaphthalene-2-carboxanilide in dimethyl sulfoxide in electrochemical microcell. *39th International Conference on Modern Electrochemical Methods (MEM),* Jetřichovice, Czech Republic (20.-24. May 2019).
11. **Gajdár J.**, Tsami K., Goněc T., Jampílek J., Brázdová M., Bábková Z., Fojta M., Barek J., Fischer J.: Electrochemical investigation of substituent effect on oxidation potentials of novel antimycobacterial agents. *52nd Heyrovsky Discussion on Electrochemistry of Organic Compounds and Biopolymers,* Liblice, Czech Republic (16.-20. June 2019).
12. **Gajdár J.**, Barek J., Fischer J.: Novel construction of renewable silver amalgam film electrode for voltammetric analysis. *15th International Students Conference on Modern Analytical Chemistry,* Prague, Czech Republic (19.-20. September 2019).

C) List of poster presentations:

1. **Gajdár J.**, Goněc T., Jampílek J., Brázdová M., Bábková Z., Fojta M., Barek J., Fischer J.: Micro volume voltammetry of a novel antimycobacterial agent at a glassy carbon electrode. *Euroanalysis 2017,* Stockholm, Sweden (28. August - 1. September 2017).
2. **Gajdár J.**, Goněc T., Jampílek J., Brázdová M., Bábková Z., Fojta M., Barek J., Fischer J.: Micro volume voltammetry of ring-substituted 1-hydroxynaphthalene-2-carboxanilides. *17th International Conference on Electroanalysis (ESEAC 2018),* Rhodes, Greece (3.-7. June 2018).
3. **Gajdár J.**, Tsami K., Goněc T., Jampílek J., Brázdová M., Bábková Z., Fojta M., Barek J., Fischer J.: Relation between biological activity, structure and voltammetric behavior of novel antimycobacterial agents. *XXV International Symposium on Bioelectrochemistry and Bioenergetics,* Limerick, Ireland (26.-30. May 2019).

D) Internships:

1. Long-term foreign internship in the laboratory of prof. Daniel Mandler, Institute of Chemistry, The Hebrew University of Jerusalem, Jerusalem, Israel (16 October 2017 – 16 January 2018).